Physics Based Modeling of Urea Selective Catalytic Reduction Systems

by

Hanbee Na

B.S. Aerospace Engineering
Korea Advanced Institute of Science and Technology, 2001

M.S. Aerospace Engineering
Korea Advanced Institute of Science and Technology, 2003

Submitted to the Department of Mechanical Engineering
in partial fulfillment of the requirement for the degree of

Master of Science in Mechanical Engineering

at the

MASSACHUSETTS INSTITUTE OF TECHNOLOGY

June 2010

Author .....
Department of Mechanical Engineering
May 13, 2010

Certified by .....
Anuradha M. Annaswamy
Senior Research Scientist
Thesis Supervisor

Accepted by .....
David E. Hardt
Chairman, Department Committee on Graduate Students

Physics Based Modeling of Urea Selective Catalytic Reduction Systems

By

Hanbee Na

Submitted to the Department of Mechanical Engineering
on May 13, 2010, in partial fulfillment of the requirements
for the degree of Master of Science in Mechanical Engineering

ABSTRACT

This thesis addresses control-oriented modeling of urea-selective catalytic reduction (SCR) after-treatment systems used for reducing NO_x emission in diesel vehicles. Starting from first-principles, appropriate simplifications are made in the underlying energy and species equations to yield simple governing equations of the Urea-SCR. The resulting nonlinear partial differential equations are discretized and linearized to yield a family of linear finite-dimensional state-space models of the SCR at different operating points. It is shown that this family of models can be reduced to three operating regions that are classified based on the relative NO_x and NH_3 concentrations. Within each region, parametric dependencies of the system on physical mechanisms are derived. A further model reduction is shown to be possible in each of the three regions resulting in a second-order linear model with sufficient accuracy. These models together with structured parametric dependencies on operating conditions set the stage for a systematic advanced control design that can lead to a high NO_x conversion efficiency with minimal peak-slip in NH_3. All model properties are validated using simulation studies of a high fidelity nonlinear model of the Urea-SCR, and compared with experimental data from a flow-reactor.

Thesis Supervisor: Anuradha M. Annaswamy

Title: Senior Research Scientist

CONTENTS

LIST OF FIGURES

LIST OF TABLES

INTRODUCTION

One of the major sources of air pollution is emission from vehicles [1], causing emission regulations to become more stringent. For example, according to U.S. Environmental Protection Agency reports, NO_x emission of diesel vehicles should less than 0.20 g/bhp-hr in their exhaust gas by the year 2010 [2]. The major emission pollutants from diesel vehicles are CO_x, unburned fuel, and NO_x, the reduction of which is carried out using three-way converters. While the efficiency of CO_x and unburned diesel fuel conversion rate is satisfactory, the efficiency of NO_x reduction is observed to drop rapidly if operating conditions vary beyond their nominal range [3]. This in turn has motivated the development of devices such as the NO_x trap [4] and the urea-SCR system, with the latter yielding NO_x conversion efficiency over 90 % [5].

In a Urea SCR, urea is first supplied from a containing tank and is in turn converted into Ammonia through pyrolysis. The gas phase Ammonia is first adsorbed onto the surface of the catalyst, and it reacts with gas-phase NO_x in exhaust gas with the aid of the catalyst. The following reaction pathway, generally referred to as standard SCR (Selective Catalytic Reaction), and referred to as *reduction* in this thesis:

$$4NH_3(s) + 4NO(g) + O_2(g) \rightarrow 6H_2O(g) + 4N_2(g)$$

In this reaction, gas phase NO_x, Oxygen, and adsorbed Ammonia react with each other to produce water and Nitrogen. This reaction occurs dynamically, and the goal of this thesis is to determine a low-order reduced order model that captures this conversion accurately, thereby

setting the stage for a control design that allows the determination of an optimal profile of the Ammonia input that allows a maximum NO_x conversion.

Dynamic models of the Urea-SCR have been addressed in [4, 6-8] in recent years. In [6, 7], the authors analyzed physical and chemical phenomena, derived one dimensional governing equations [7], and converted it into state space form models with three state variables, θ (NH_3 loading fraction), gas-phase concentration of Ammonia, and Oxides Nitrogen. A linear spatial variation in the NO_x and NH_3 concentrations is assumed. However, in this thesis, the gas-phase concentration of Ammonia and oxides Nitrogen are not treated as state variables, because their effects were found to be small compared to θ.

The approach in [8] used system identification, with an assumption that the underlying system is first-order. The corresponding parameters were determined using a system-identification procedure and experiments over a range of operating conditions. A systems-identification approach is used in [4] as well, where a first-order plant with nonlinear gains is derived as the underlying SCR model. Using the responses of the high-fidelity nonlinear model in [5], effects of a number of mechanisms including chemical reactions, exhaust gas dynamics, and heat exchange between exhaust gas and catalyst are included in their model.

In this thesis, a first-principles based control-oriented reduced order model of the Urea-SCR is derived. Appropriate simplifications are made in the underlying energy and species equations to yield simple governing equations of the Urea-SCR. The resulting nonlinear partial differential equations are discretized and linearized to yield a family of linear finite-dimensional state-space models of the SCR at different operating points. It is shown that this family of models can be reduced to three operating regions that are classified based on the relative NO_x and NH_3 concentrations. Within each region, parametric dependencies of the system on

physical mechanisms are derived. A further model reduction is shown to be possible in each of the three regions resulting in a second-order linear model with sufficient accuracy. These models together with structured parametric dependencies on operating conditions set the stage for a systematic advanced control design that can lead to a high NO_x-conversion efficiency with minimal peak-slip in NH_3. All model properties are validated using simulation studies of a high fidelity nonlinear model of the Urea-SCR, and compared with experimental data from a flow-reactor.

NONLINEAR MODEL

PHYSICAL AND CHEMICAL PHENOMENA IN THE CATALYST

The catalyst is assumed to have a honeycomb structure, with a circular cross-section. As shown in Figure 1 [7], each channel consists of monolith, washcoat, and void space. The monolith supports the catalyst, and is made of Aluminum-Oxide, and the catalyst material is Copper-Zeolite. The washcoat layer is of a porous medium, thereby allowing diffusion of molecules between stationary gas in the porous medium and flowing gas in the channel. When exhaust gas containing NH_3 and NO_x is supplied into the channel, several physical and chemical phenomena occur. The first phenomenon is a diffusion of species of NH_3 and NO_x between flowing gas and stationary gas in wash coat which is then followed by chemical reaction between molecules on the surface of the catalyst. The third phenomenon is heat transfer among the flowing gas, the stationary gas in washcoat, and structure. To model these phenomena, we need at least three energy equations of flow gas, gas in the wash coat, and the structure, and species equations for each species in flowing channel, in stationary gas of wascoat, and on the catalyst.

Equation (1) and (2) are energy equations to calculate wall temperature and gas temperature.

$$\rho_w A_w C_{P,w} \frac{\partial T_w}{\partial t} = -h \cdot P(T_w - T_g) + s \sum_j R_j \Delta H_j \tag{1}$$

$$\rho_g A_g C_{P,g} \frac{\partial T_g}{\partial t} + \rho_g A_g C_{P,g} u \frac{\partial T_g}{\partial x} = -h \cdot P(T_g - T_w) \tag{2}$$

where, subscript $_j$ denotes the j'th reaction-pathway, and A_w and A_g are cross-section area of wall and void channel, respectively. In Equation (1), heat conduction in axial direction is

neglected, because this is generally assumed to be small compared to convective heat exchange term.

Equation (3), (4), and (5) represent equations of the i'th species in the flowing gas, and the stationary gas in washcoat, and on the catalyst surface, respectively.

$$A_g \frac{\partial C_i}{\partial t} + A_g u \frac{\partial C_i}{\partial x} = -D \cdot P\left(C_i - C_{i(wt)}\right) \tag{3}$$

$$A_{wt} \frac{\partial C_{i(wt)}}{\partial t} = D \cdot P\left(C_i - C_{i(wt)}\right) - s\sum_j R_{j,i} \tag{4}$$

$$A_w \frac{\partial C_{i(s)}}{\partial t} = s\sum_j R_{j,i} \tag{5}$$

where, subscript $_i$ corresponds to the i'th species, and subscript $_j$ denotes the j'th reaction-pathway.

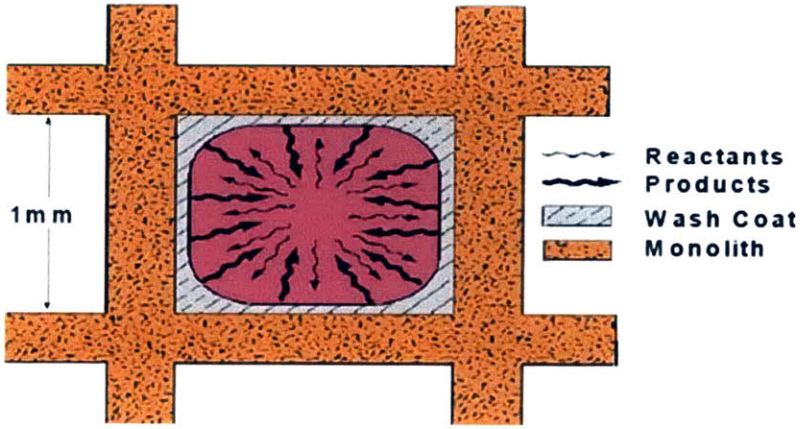

Figure 1 Top view of each channel of the urea-SCR with a honeycomb structure ([8])

CHEMICAL REACTIONS

The Eley-Rideal mechanism is used to consider chemical reactions on the surface of the catalyst. According to this mechanism, only gas Ammonia molecules are able to be adsorbed onto the surface of the catalyst, and the adsorbed Ammonia reacted with gas phase other species. This is shown in Figure 2, where "B" denotes adsorbed Ammonia, and "A" denotes other species such as NO and O_2, and "C" refers to product molecules.

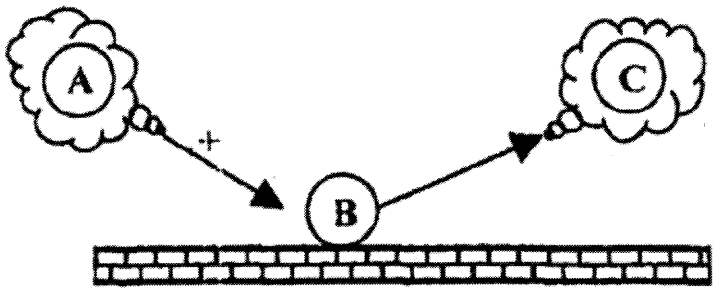

Figure 2 Eley-Rideal mechanism ([7])

To simplify the model, only four dominant reaction pathways such as adsorption, desorption, reduction, and oxidation (Equations (6), (7), (8), and (9)) are included [7]. The first reaction is adsorption, where gas phase Ammonia molecules are adsorbed onto the surface of the catalyst. The second reaction considered is desorption which means that the adsorbed Ammonia molecules are detached from the surface of the catalyst. The third reaction is reduction, which is standard SCR, in which the adsorbed Ammonia reacts with gas phase Nitrogen Monoxide (NO) and they are converted to water and Nitrogen. The last considered reaction is oxidation which means that adsorbed Ammonia reacts with gas-phase Oxygen in the flowing gas. It is observed

that the effect of oxidation is negligible when catalyst temperature is less than 200 °C.

$$NH_3(g) \longrightarrow NH_3(s) \tag{6}$$

$$NH_3(s) \longrightarrow NH_3(g) \tag{7}$$

$$4NH_3(s) + 4NO(g) + O_2(g) \rightarrow 6H_2O(g) + 4N_2(g) \tag{8}$$

$$4NH_3(s) + 3O_2(g) \rightarrow 2N_2(g) + 6H_2O(g) \tag{9}$$

Reaction rates of each reaction pathway (Equation (6) to (9)) can be calculated from Equations (10) to (13). The activation energy of adsorption is assumed to be zero [5], i.e, it has no temperature dependency. The concentration of Oxygen is much higher than that of NH_3 and NO, and hence treated as balanced molecules [5], thus the concentration of Oxygen is not included in the reaction equations.

$$R_a = k_a C_{NH_3} (1-\theta) \tag{10}$$

$$R_d = k_d \exp\left(-\frac{E_{a,d}(1-\alpha\theta)}{RT_w}\right)\theta \tag{11}$$

$$R_r = k_r \exp\left(-\frac{E_{a,r}}{RT_w}\right) C_{NO}\theta \tag{12}$$

$$R_o = k_o \exp\left(-\frac{E_{a,o}}{RT_w}\right)\theta \tag{13}$$

SIMPLIFICATIONS AND ASSUMPTIONS

To make the model simpler while keeping accuracy, the following assumptions and simplification are made:

1. All channels are identical geometrically.
2. All channels are identical thermally assuming no heat loss to ambient.

   - From assumption 1 and 2, one channel model represents entire other channels.
3. Channel shape is assumed to be circular, with a one-dimensional laminar flow.
4. Flow is fully developed.
5. NO_x consists of only NO, so the minor reactions related to N_2O, NO_2 are neglected.
6. Chemical reactions in gas phase are negligible.

   - From assumption 5 and 6, reaction pathways from Equation (14) to (18) which are considered in [5] can be neglected.

$$4NH_3(s) + 2NO + 2NO_2 \rightarrow 4N_2 + 6H_2O \tag{14}$$

$$4NH_3(s) + 4O_2 \rightarrow 2N_2O + 6H_2O \tag{15}$$

$$2NH_3(s) + 2NO_2 \rightarrow N_2O + N_2 + 3H_2O \tag{16}$$

$$4NH_3(s) + 4NO + 3O_2 \rightarrow 4N_2O + 6H_2O \tag{17}$$

$$2NO + O_2 \leftrightarrow 2NO_2 \tag{18}$$

7. Storage terms such as $\rho_g A_g C_{P,g} \frac{\partial T_g}{\partial t}$ are negligible, because the heat capacity of the catalyst is much higher than the heat capacity of gas. Similarly, storage term

like $A_g \frac{\partial C_i}{\partial t}$ is negligible. Therefore, concentrations of molecules in gas phase are not treated as state variables unlike the other model [7].

8. Heat generation from chemical reaction is negligible, because the concentration of NH_3 and NO is small, and hence their heat generation is assumed to be small compared to convective heat transfer.

9. Because diffusion rate is much higher compared chemical reaction, concentration of stationary gas in washcoat is the same as that of the flowing gas. Equation (4) is therefore neglected, and Equations (3) and (5) are connected directly.

10. Heat conduction in the wall in axial direction is negligible compared to convective heat transfer.

GOVERNING EQUATIONS

From the above assumptions, governing equations which can describe the chemical and physical phenomena in the catalyst are derived. Equation (19) and (20) are the energy equations of wall and gas, respectively.

$$\frac{\partial T_g}{\partial x} = -\frac{h \cdot P}{\rho_g A_g C_{P,g} u}(T_g - T_w) \tag{19}$$

$$\frac{\partial T_w}{\partial t} = -\frac{h \cdot P}{\rho_w A_w C_{P,w}}(T_w - T_g) \tag{20}$$

Equation (21) and (22) are NH_3 and NO species equations of flowing gas in a channel.

$$\frac{\partial C_{NH_3}}{\partial x} = \frac{s}{A_g u}(-R_a + R_d) = \frac{s}{A_g u}\left(-p_a(1-\theta)C_{NH_3} + p_d \exp(-\frac{E_{d0}(1-\alpha\theta)}{R \cdot T_w})\theta\right) \tag{21}$$

$$\frac{\partial C_{NO}}{\partial x} = \frac{s}{A_g u}(-R_r) = \frac{s}{A_g u}\left(-p_r \exp(-\frac{E_r}{R \cdot T_w}) \cdot \theta \cdot C_{NO}\right) \tag{22}$$

Equation (23) is species equation of adsorbed Ammonia on the surface of catalyst. θ is fraction loading of Ammonia onto the catalyst and defined by $\frac{C_{NH_3}(s)}{\Omega}$ in which Ω is the number of reaction-sites per volume of washcoat.

$$\begin{aligned}\frac{\partial \theta}{\partial t} &= (R_a - R_d - R_r - R_o) \\ &= \left(p_a(1-\theta)C_{NH_3} - p_d \exp\left(-\frac{E_{d0}(1-\alpha\theta)}{R \cdot T_w}\right)\theta - p_r \exp\left(-\frac{E_r}{R \cdot T_w}\right) \cdot \theta \cdot C_{NO} - p_o \exp\left(-\frac{E_o}{R \cdot T_w}\right) \cdot \theta \cdot C_{O_2}\right)\end{aligned} \tag{23}$$

The reaction parameters such as activation energies and pre-exponential constants in governing equations (23) are not known *a priori,* for the catalyst. We outline below how these parameters can be determined using a limited-data set from a judiciously carried out set of experiments.

DETERMINATION OF REACTION PARAMETERS

Because the Cu-Zeolite catalyst coated onto the reactor is newly developed by the catalyst supplier, there is no reaction parameters data in the literature. A few experiments were therefore carried out to judge the performance of the catalyst and to get reaction parameters using a flow reactor with a diameter and length around 1 inch (see Figure 3 for a schematic). In the underlying model in [5], seven reaction pathways are considered, corresponding to which thirteen unknown reaction parameters are present (assuming zero activation energy of adsorption), which are obtained from the experiments.

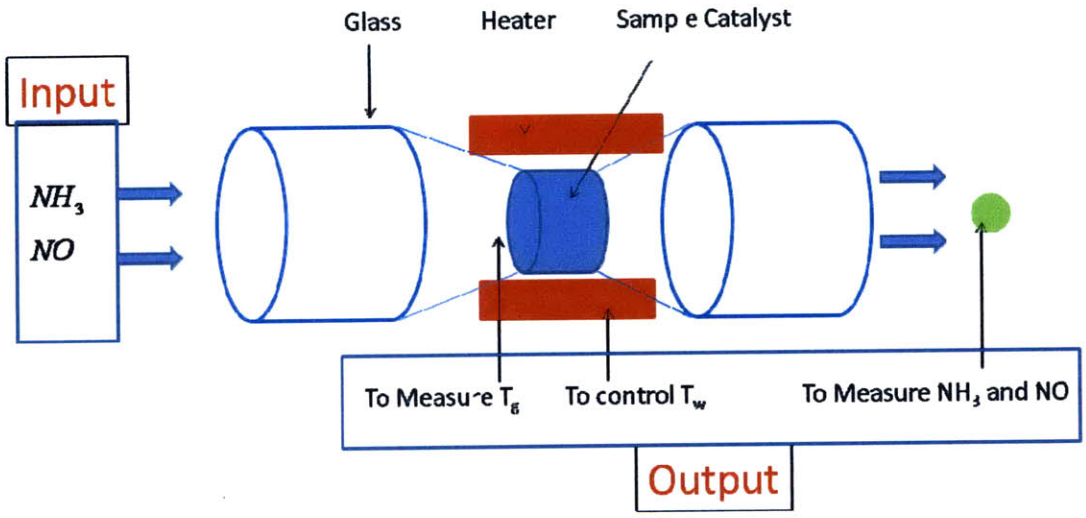

Figure 3 A schematic of a sample-size reactor experiments

In the model developed in this thesis, we used four reaction pathways, adsorption, desorption, reduction, and oxidation, so there are seven unknown parameters like four pre-exponential parameters p_a, p_d, p_r, p_o and three activation energies E_{d0}, E_r, E_o assuming zero

activation energy of adsorption.

We separately obtained seven reaction parameters based the sample experiments. The basic procedure used for the parameter estimation consists of three steps, each of which is described below.

1) Obtain reaction parameters related to adsorption and desorption (p_a, p_r, and E_{d0})

In step one, a temperature programmed desorption (TPD) experiment was carried out in which a fixed concentration Ammonia is supplied to the reactor at fixed temperature for some time, and NO_x is not supplied during whole experiment, then the Ammonia supply is stopped to see desorption of the reactor. Then, the temperature is increased to promote desorption of the catalyst. Figure 4 is an example of TPD experiment [9], where $V_2O_5 - WO_3 / TiO_2$ is used as catalyst material. The top plot of Figure 4 is TDP experiment when an initial reactor temperature is 493 K. Only Ammonia is supplied from 0 sec to around 750 sec, and initial stage, there is no Ammonia slip, because all of the supplied Ammonia is adsorbed onto the catalyst. Then, the Ammonia slip reaches to the same concentration of input Ammonia concentration, because the catalyst is saturated. Around 750 sec, Ammonia supply is stop, so Ammonia slip is only due to desorption of Ammonia which are adsorbed onto the catalyst. Until around 1600 sec, the reactor temperature is fixed at 493 K, but the reactor temperature is increased after then to promote desorption of Ammonia.

These experiments were repeated for various initial reactor temperatures, with the data corresponding to an initial temperature of 423 K used to get the three parameters in step 1. In this experiment, we did not consider reaction parameters related reduction (p_r and E_r) because there is no supply of NO_x, and we also did not consider reaction parameters related oxidation

(p_o and E_o) because oxidation is not dominant at low reactor temperature.

An iteration method and least square method were used to get three parameters. First p_d and E_{d0} are set at arbitrary values, and the simulations are carried out using the same experimental input conditions until the catalyst is saturated with Ammonia. Then, we obtained p_a which minimize E^* defined as

$$E^* = \int_{0\,\mathrm{sec}}^{A} \left(C_{NH_3,out,ex}(t) - C_{NH_3,out,sim}(t) \right)^2 dt \tag{24}$$

where, subscript ex and sim are experimental data and simulation results, respectively, using a least square method where A denotes the time at which the catalyst is saturated. We then compared the experimental and simulation data from A to the end of experiment for the obtained p_a, p_d and E_{d0} were determined to minimize E^{**} which is defined as

$$E^{**} = \int_{A}^{end} \left(C_{NH_3,out,ex}(t) - C_{NH_3,out,sim}(t) \right)^2 dt \tag{25}$$

We repeated this procedure to get more accurate parameters.

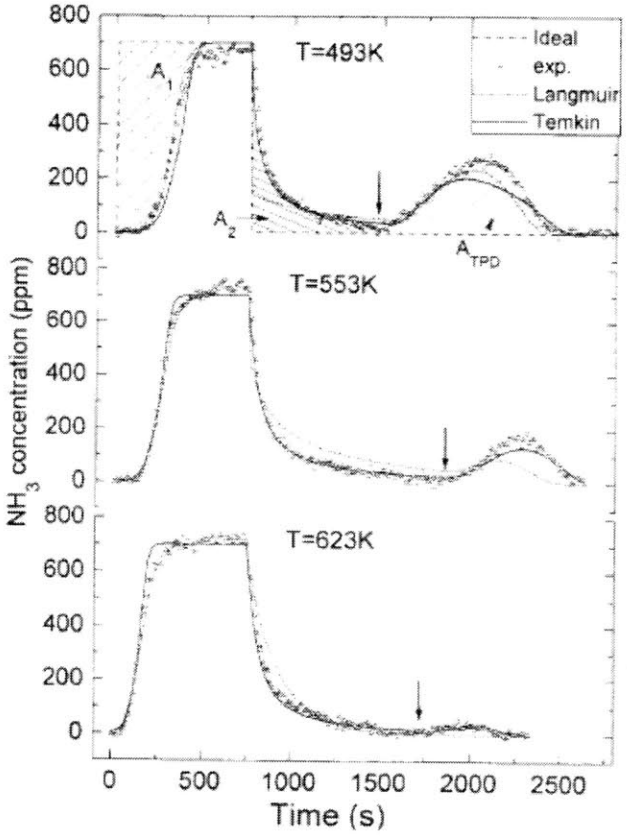

Figure 4 Examples of TPD experiment ([9])

2) Obtain reaction parameters related to oxidation (p_o and E_o)

TPD experiments with higher initial reactor temperatures were used to obtain p_o and E_o. We found that if the wall temperature is higher than 200 °C, then oxidation effect become dominant, so the Ammonia slip concentration under saturation condition is less than Ammonia input condition. In [9], this phenomenon was not observed which may be due to the fact that a different kind of catalyst was used in their studies.

For the obtained parameters p_a, p_d, and E_{d0}, two unknown parameters p_o and E_o

were obtained to minimize E^*.

$$E^* = \sum_{T_w} \left(C_{NH3,out,ex,sat} - C_{NH3,out,sim,sat} \right)^2 \tag{26}$$

where the subscription $_{sat}$ is the concentration when the catalyst is saturated with Ammonia. The TPD results the with initial temperatures of 200, 250, 300, 350, 400, 450, 500, and 550 ^{o}C were used to get E^*.

3) Obtain reaction parameters related to reduction (p_r and E_r)

To get reaction parameters p_r and E_r, the same concentration of NO to Ammonia were supplied for several fixed reactor temperature. Because reduction of NO occurs inside the reactor, the output concentration of Nitrogen Monoxide $C_{NO,out}$ is lower than input concentration $C_{NO,in}$. Parameters p_r and E_r were obtained to minimize

$$E^* = \sum_{T_w} \left(C_{NO,out,ex} - C_{NO,out,sim} \right)^2 \tag{27}$$

This experiment was conducted for reactor temperatures of 175, 200, 225, 250, 275, 300, 325, 350, 400, 450, and 500 ^{o}C.

VALIDATION

Flow reactor experiments were carried out with a reactor setup with a diameter and length around 1 inch (see Figure 3 for a schematic). The input concentration of NH_3 and NO were adjusted by controlling the supply pressure of NH_3 and NO and the temperature of reactor was controlled using a heater. The experimental input conditions are shown in Figure 5, where the black and red plots correspond to input concentrations of NO, and NH_3, respectively. The experiments were conducted for various temperature ranges from 500 °C to 300 °C with 100 °C intervals and from 300 °C to 200 °C with 50 °C intervals. The space velocity was fixed at 30,000 /Hr.

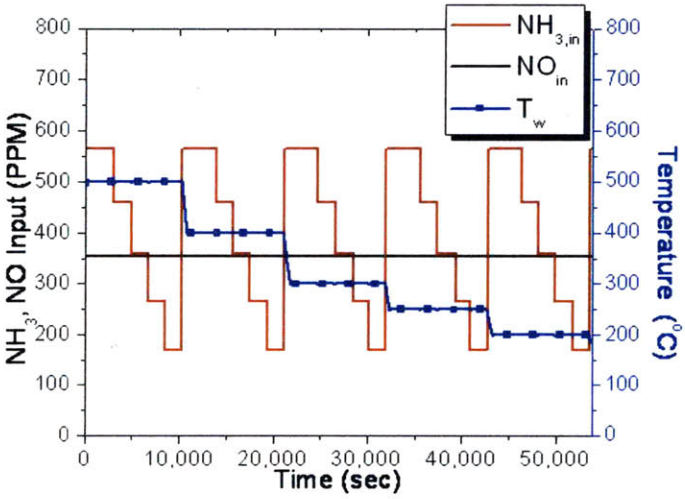

Figure 5 Input conditions for reactor experiment

The resulting output concentrations of NH_3 and NO from the experimental studies are shown in Figure 6 (black line) and Figure 7 (black line). The same input condition in Figure 5 was plugged into the model described in Equations (19) to (23), and the output concentration of NH_3 and NO were obtained (red line in Figure 6 and Figure 7) and compared with the experimental data in Figure 6 and Figure 7. These results show a good agreement between the model prediction and experiments except at very low and very high temperatures. The reason for the discrepancy at high temperatures may be due to the fact that the reaction parameters in Equations (21) to (23) were determined using the experimental data that was somewhat limited in the high temperature range. The reason for the discrepancy at low temperatures may be due to that the fact that some of underlying assumptions are not suitable. However, the nominal operating temperature is usually between 225 °C to 300 °C, during which range the NO_x conversion rate is over 90 %, where the accuracy of the proposed model is high. Therefore, we concluded that this model and its underlying assumptions are reasonable for most operating conditions.

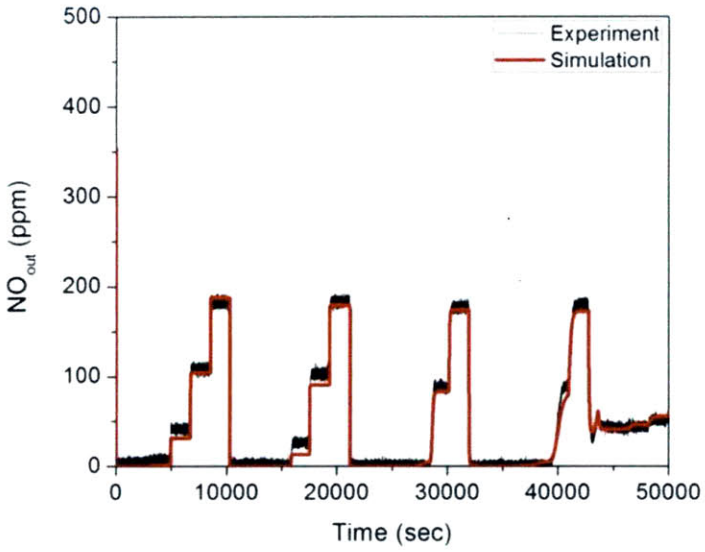

Figure 6 Comparison of NO output concentration

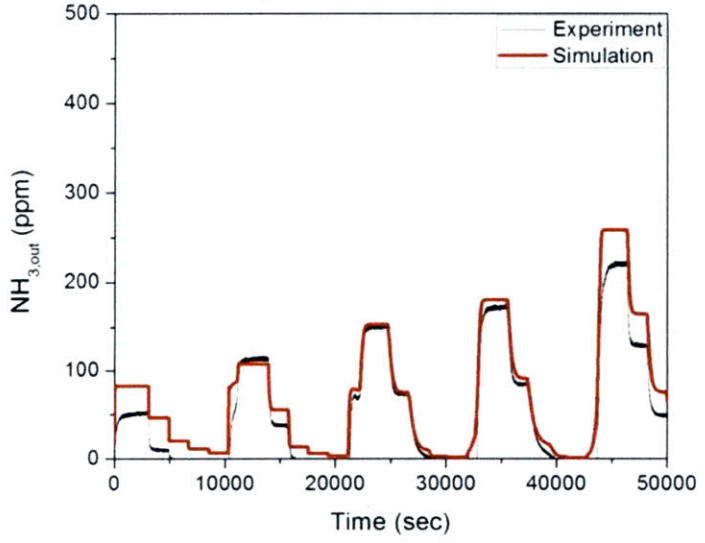

Figure 7 Comparison of NH3 output concentration

LINEARIZED MODEL

As seen in the above discussions, the underlying model, described in Equations (19) to (23), is a spatial-temporal, nonlinear, partial differential equation (PDE). In this chapter, we derive a linear finite-dimensional model starting from Equations (19) to (23).

To derive state space form for the whole system, we first discretized equations in spatial domain, and derived state space form equation for governing Equations (20) and (23) which is continuous in time for each segment. Then, every state equation for each segment is assembled into one large state space equation.

DISCRETIZATION IN SPACE

To derive the reactor's state space equation, the reactor is first discretized in axial direction as in Figure 8 in which inputs, output, and state variables for a segment are shown. Equations (21), (22), and (19) that pertain to spatial derivates are discretized spatially, but governing Equations (23) and (20) is still in the continuous form after discretization.

Equations (21), (22), and (19) which are governing equations for C_{NH3}, C_{NO}, and T_g are discretized in the axial direction (x direction in the equations). In this procedure, the state variables θ_i and $T_{w,i}$ are assumed to be constant in each segment.

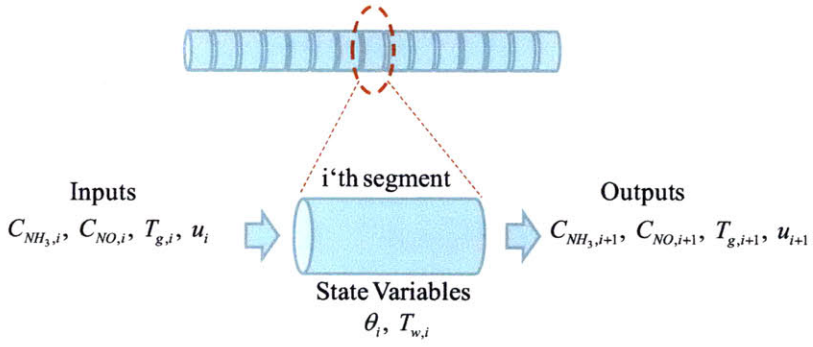

Figure 8 Inputs, outputs, and state varibles of each segment

Using the first-order implicit Euler method, gas temperature output of i'th segment can be expressed as

$$\frac{T_{g,i+1}-T_{g,i}}{\Delta x}=T_{g,i}-\frac{h\cdot P}{\rho_g A_g C_{P,g} u}\left(T_{g,i+1}-T_{w,i}\right) \tag{28}$$

where subscription $_i$ is an index for segmentation, and state variable $T_{w,i}$ is assumed to be a constant in the i'th segment. Therefore, gas temperature output of i'th segment is expressed as follows:

$$T_{g,i+1} = \left(\frac{\rho_g A_g C_{p,g} u}{\rho_g A_g C_{p,g} u + h \cdot P \cdot \Delta x} \right) \cdot T_{g,i} + \left(\frac{h \cdot P \cdot \Delta x}{\rho_g A_g C_{p,g} u + h \cdot P \cdot \Delta x} \right) \cdot T_{w,i} \tag{29}$$

Similarly, discretized form of the species equations of gas-phase Ammonia and Nitrogen Monoxide (Equations (21) and (22)) are expressed as

$$C_{NH_3,i+1} = \frac{A_g u}{A_g u + s\Delta x \cdot p_a \cdot (1-\theta_i)} C_{NH_3,i} + \frac{s \cdot \Delta x \cdot p_d}{A_g u + s\Delta x \cdot p_a \cdot (1-\theta_i)} \exp\left(\frac{-E_{d0}(1-\alpha\theta_i)}{R \cdot T_w} \right) \cdot \theta_i \tag{30}$$

$$C_{NO,i+1} = \frac{A_g u}{A_g u + s \cdot \Delta x \cdot p_r \cdot \exp\left(-\frac{E_r}{R \cdot T_{w,i}} \right) \cdot \theta_i} C_{NO,i} \tag{31}$$

Equations (23) and (20), after discretization, are expressed as

$$\begin{aligned} \frac{\partial \theta_i}{\partial t} &= \left(R_{a,i} - R_{d,i} - R_{r,i} - R_{o,i} \right) \\ &= \left(p_a (1-\theta) C_{NH_3,i} - p_d \exp\left(-\frac{E_{d0}(1-\alpha\theta_i)}{R \cdot T_{w,i}} \right) \theta_i - p_r \exp\left(-\frac{E_r}{R \cdot T_{w,i}} \right) \cdot \theta_i \cdot C_{NO,i} - p_o \exp\left(-\frac{E_o}{R \cdot T_{w,i}} \right) \cdot \theta_i \cdot C_{O_2} \right) \end{aligned} \tag{32}$$

$$\frac{\partial T_{w,i}}{\partial t} = -\frac{h \cdot P}{\rho_w A_w C_{P,w}} (T_{w,i} - T_{g,i}) \tag{33}$$

LINEARIZATION

From now, three of five governing equations are in discretized form in the space domain, and the rest are in continuous form in time domain. Table 1 compares five governing equations before and after discretization.

Table 1 Governing equations before and after discretization

Before Discretization for whole reactor	After Discretization for each segment
$\frac{\partial\theta}{\partial t}=\left(R_a-R_d-R_r-R_o\right)$ (23)	$\frac{\partial\theta_i}{\partial t}=\left(R_{a,i}-R_{d,i}-R_{r,i}-R_{o,i}\right)$ (32)
$\frac{\partial T_w}{\partial t}=-\frac{h\cdot P}{\rho_w A_w C_{P,w}}(T_w-T_g)$ (20)	$\frac{\partial T_{w,i}}{\partial t}=-\frac{h\cdot P}{\rho_w A_w C_{P,w}}(T_{w,i}-T_{g,i})$ (33)
$\frac{\partial C_{NH_3}}{\partial x}=\frac{s}{A_g u}\left(-p_a(1-\theta)C_{NH_3}+p_d\exp(-\frac{E_{d0}(1-\alpha\theta)}{R\cdot T_w})\theta\right)$ (21)	$C_{NH_3,i+1}=\frac{A_g u}{A_g u+s\Delta x\cdot p_a\cdot(1-\theta_i)}C_{NH_3,i}+\frac{s\cdot\Delta x\cdot p_d}{A_g u+s\Delta x\cdot p_a\cdot(1-\theta_i)}\exp\left(\frac{-E_{d0}(1-\alpha\theta_i)}{R\cdot T_w}\right)\cdot\theta_i$ (30)
$\frac{\partial C_{NO}}{\partial x}=\frac{s}{A_g u}\left(-p_r\exp(-\frac{E_r}{R\cdot T_w})\cdot\theta\cdot C_{NO}\right)$ (22)	$C_{NO,i+1}=\frac{A_g u}{A_g u+s\cdot\Delta x\cdot p_r\cdot\exp\left(-\frac{E_r}{R\cdot T_{w,i}}\right)\cdot\theta_i}C_{NO,i}$ (31)
$\frac{\partial T_g}{\partial x}=-\frac{h\cdot P}{\rho_g A_g C_{P,g} u}(T_g-T_w)$ (19)	$T_{g,i+1}=\left(\frac{\rho_g A_g C_{p,g} u}{\rho_g A_g C_{p,g} u+h\cdot P\cdot\Delta x}\right)\cdot T_{g,i}+\left(\frac{h\cdot P\cdot\Delta x}{\rho_g A_g C_{p,g} u+h\cdot P\cdot\Delta x}\right)\cdot T_{w,i}$ (29)

Next step is to linearize the five governing equations, two of which are continuous in time domain and three of which are discretized in the space, around an equilibrium point that is determined using nominal input conditions. The equilibrium point for each segment i is determined by $C_{NH_3,i,eq}$, $C_{NO,i,eq}$, $\theta_{i,eq}$, $T_{w,i,eq}$, $T_{g,i,eq}$, and $u_{i,eq}$. These in turn are determined by supplying a constant $C_{NH_3,in}$, $C_{NO,in}$, $T_{g,in}$, and $u_{in,eq}$ with the resulting steady-state values of

the i'th segment set as the corresponding equilibrium point. Using these equilibrium points, Equations (32) and (33) can be linearized around equilibrium points as follows:

$$\frac{\partial(\delta\theta_i)}{\partial t} = J_{11,i}\cdot\delta\theta_i + J_{12,i}\cdot\delta T_{w,i} + J_{13,i}\cdot\delta C_{NH_3,i} + J_{14,i}\cdot\delta C_{NO,i} \tag{34}$$

$$\frac{\partial(\delta T_{w,i})}{\partial t} = J_{22,i}\delta T_{w,i} + J_{25,i}\delta T_{g,i} \tag{35}$$

where $J_{kl,i}$ means that partial derivative of a k'th index variable with respect to l'th index variable under equilibrium in i'th segment. Variables indexed by k and l include the following:

1: θ

2: T_w

3: C_{NH3}

4: C_{NO}

5: T_g

6: u

From Equations (34) and (35), system matrix for the i'th segment can be expressed as follows:

$$\frac{d}{dt}\begin{pmatrix}\delta\theta_i\\ \delta T_{w,i}\end{pmatrix}=\begin{bmatrix}J_{11,i} & J_{12,i}\\ 0 & J_{22,i}\end{bmatrix}\begin{pmatrix}\delta\theta_i\\ \delta T_{w,i}\end{pmatrix}+\begin{bmatrix}J_{13,i} & J_{14,i} & 0 & 0\\ 0 & 0 & J_{25,i} & 0\end{bmatrix}\begin{pmatrix}\delta C_{NH3,i}\\ \delta C_{NO,i}\\ \delta T_{g,i}\\ \delta u_i\end{pmatrix} \tag{36}$$

This is in turn,

$$\dot{\mathbf{x}}_i = \mathbf{A}_i\mathbf{x}_i + \mathbf{B}_i\mathbf{u}_i \tag{37}$$

where, $\mathbf{x}_i=\begin{pmatrix}\delta\theta_i\\ \delta T_{w,i}\end{pmatrix}$, $\mathbf{A}_i=\begin{bmatrix}J_{11,i} & J_{12,i}\\ 0 & J_{22,i}\end{bmatrix}$, $\mathbf{B}_i=\begin{bmatrix}J_{13,i} & J_{14,i} & 0 & 0\\ 0 & 0 & J_{25,i} & 0\end{bmatrix}$, and $\mathbf{u}_i=\begin{pmatrix}\delta C_{NH3,i}\\ \delta C_{NO,i}\\ \delta T_{g,i}\\ \delta u_i\end{pmatrix}$.

In order to obtain the output equation for the *i*'th segment, governing Equations (30), (31), and (29) should be linearized around equilibrium point as follows:

$$\begin{aligned}\delta C_{NH_3,i+1} &= \frac{\partial C_{NH_3,i+1}}{\partial\theta_i}\delta\theta_i + \frac{\partial C_{NH_3,i+1}}{\partial T_{w,i}}\delta T_{w,i} + \frac{\partial C_{NH_3,i+1}}{\partial C_{NH_3,i}}\delta C_{NH_3,i} + \frac{\partial C_{NH_3,i+1}}{\partial u}\delta u\\ &= J_{31,i}\delta\theta_i + J_{32,i}\delta T_{w,i} + J_{33,i}\delta C_{NH_3,i} + J_{36,i}\delta u\end{aligned} \tag{38}$$

$$\begin{aligned}\delta C_{NO,i+1} &= \frac{\partial C_{NO,i+1}}{\partial\theta_i}\delta\theta_i + \frac{\partial C_{NO,i+1}}{\partial T_{w,i}}\delta T_{w,i} + \frac{\partial C_{NO,i+1}}{\partial C_{NO,i}}\delta C_{NO,i} + \frac{\partial C_{NO,i+1}}{\partial u}\delta u\\ &= J_{41,i}\delta\theta_i + J_{42,i}\delta T_{w,i} + J_{44,i}\delta C_{NO,i} + J_{46,i}\delta u\end{aligned} \tag{39}$$

$$\delta T_{g,i+1} = \frac{\partial T_{g,i+1}}{\partial T_{w,i}}\delta T_{w,i} + \frac{\partial T_{g,i+1}}{\partial T_{g,i}}\delta T_{g,i} + \frac{\partial T_{g,i+1}}{\partial u_i}\delta u_i \tag{40}$$

The output equations can be summarized from Equations (38), (39), and (40) as follows:

$$\begin{pmatrix} \delta C_{NH_3,i+1} \\ \delta C_{NO,i+1} \\ \delta T_{g,i+1} \\ \delta u_{i+1} \end{pmatrix} = \begin{bmatrix} J_{31,i} & J_{32,i} \\ J_{32,i} & J_{32,i} \\ 0 & J_{33,i} \\ 0 & 0 \end{bmatrix} \begin{pmatrix} \delta\theta_i \\ \delta T_{w,i} \end{pmatrix} + \begin{bmatrix} J_{33,i} & 0 & 0 & J_{36,i} \\ 0 & J_{34,i} & 0 & J_{46,i} \\ 0 & 0 & J_{35,i} & J_{55,i} \\ 0 & 0 & 0 & 1 \end{bmatrix} \begin{pmatrix} \delta C_{NH_3,i} \\ \delta C_{NO,i} \\ \delta T_{g,i} \\ \delta u_i \end{pmatrix} \tag{41}$$

This is in turn expressed compactly as

$$\mathbf{y_i} = \mathbf{C_i x_i} + \mathbf{D_i u_i} \tag{42}$$

where

$$\mathbf{y_i} = \begin{pmatrix} \delta C_{NH_3,i+1} \\ \delta C_{NO,i+1} \\ \delta T_{g,i+1} \\ \delta u_{i+1} \end{pmatrix}, \quad \mathbf{x_i} = \begin{pmatrix} \delta\theta_i \\ \delta T_{w,i} \end{pmatrix}, \quad \mathbf{u_i} = \begin{pmatrix} \delta C_{NH3,i} \\ \delta C_{NO,i} \\ \delta T_{g,i} \\ \delta u_i \end{pmatrix}, \quad \mathbf{C_i} = \begin{bmatrix} J_{31,i} & J_{32,i} \\ J_{32,i} & J_{32,i} \\ 0 & J_{33,i} \\ 0 & 0 \end{bmatrix}, \text{ and } \mathbf{D_i} = \begin{bmatrix} J_{33,i} & 0 & 0 & J_{36,i} \\ 0 & J_{34,i} & 0 & J_{46,i} \\ 0 & 0 & J_{35,i} & J_{55,i} \\ 0 & 0 & 0 & 1 \end{bmatrix}.$$

The Jacobians $J_{lk,i}$ are given in Appendix A.

STATE SPACE EQUATION FOR THE ENTIRE SYSTEM

After we first carried out a discretization and linearization procedure to convert the nonlinear PDEs (Equations (19) to (23)) into the linear system (Equations (37) and (42)), we assembled state space equations for each segment into a single, large, state space equation. External inputs include $C_{NH_3,in}$, $C_{NO,in}$, $T_{g,in}$, and u_{in}, the inputs to the first segment, while system outputs are the outputs of the N'th segment, and are denoted as $C_{NH_3,out}$, $C_{NO,out}$, and $T_{g,out}$. Gas velocity is assumed to be uniform for the sake of simplicity. It was observed that a choice of N=15 resulted in sufficient accuracy, leading to a 30^{th} order linear system.

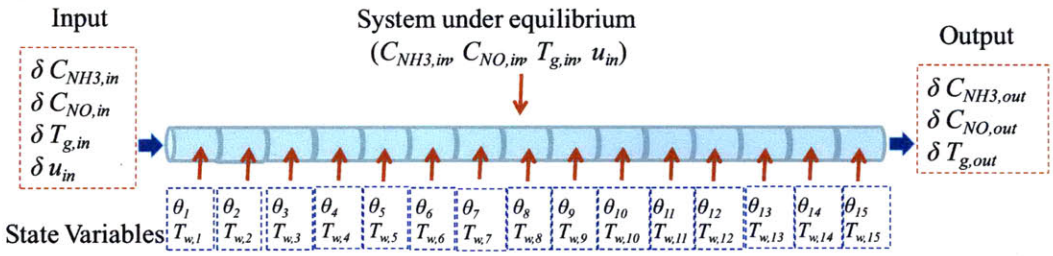

Figure 9 Discretization of a catalyst block, input and output variables, and state variables

First we placed every state space equation into one state space equations as follows:

$$\frac{d}{dt}\begin{pmatrix}\mathbf{x}_1\\ \mathbf{x}_2\\ \mathbf{x}_3\\ \mathbf{x}_4\\ \mathbf{x}_5\\ \cdot\\ \mathbf{x}_{12}\\ \mathbf{x}_{13}\\ \mathbf{x}_{14}\\ \mathbf{x}_{15}\end{pmatrix} = \begin{pmatrix}\mathbf{A}_1 & & & & & & & & & & & & & & \\ & \mathbf{A}_2 & & & & & & & & & & & & & \\ & & \mathbf{A}_3 & & & & & & & & & & & & \\ & & & \mathbf{A}_4 & & & & & & & & & & & \\ & & & & \mathbf{A}_5 & & & & & & & & & & \\ & & & & & \cdot & & & & & & & & & \\ & & & & & & \mathbf{A}_{12} & & & & & & & & \\ & & & & & & & \mathbf{A}_{13} & & & & & & & \\ & & & & & & & & \mathbf{A}_{14} & & & & & & \\ & & & & & & & & & \mathbf{A}_{15} & & & & & \end{pmatrix}\begin{pmatrix}\mathbf{x}_1\\ \mathbf{x}_2\\ \mathbf{x}_3\\ \mathbf{x}_4\\ \mathbf{x}_5\\ \cdot\\ \mathbf{x}_{12}\\ \mathbf{x}_{13}\\ \mathbf{x}_{14}\\ \mathbf{x}_{15}\end{pmatrix} + \begin{pmatrix}\mathbf{B}_1 & & & & & & & & & & & & & & \\ & \mathbf{B}_2 & & & & & & & & & & & & & \\ & & \mathbf{B}_3 & & & & & & & & & & & & \\ & & & \mathbf{B}_4 & & & & & & & & & & & \\ & & & & \mathbf{B}_5 & & & & & & & & & & \\ & & & & & \cdot & & & & & & & & & \\ & & & & & & \mathbf{B}_{12} & & & & & & & & \\ & & & & & & & \mathbf{B}_{13} & & & & & & & \\ & & & & & & & & \mathbf{B}_{14} & & & & & & \\ & & & & & & & & & \mathbf{B}_{15} & & & & & \end{pmatrix}\begin{pmatrix}\mathbf{u}_1\\ \mathbf{u}_2\\ \mathbf{u}_3\\ \mathbf{u}_4\\ \mathbf{u}_5\\ \cdot\\ \mathbf{u}_{12}\\ \mathbf{u}_{13}\\ \mathbf{u}_{14}\\ \mathbf{u}_{15}\end{pmatrix} \tag{43}$$

Because every segment is connected by input and output, Equation (43) can be expressed in terms of the system input

$$\mathbf{u} = \begin{pmatrix}\delta C_{NH3,in}\\ \delta C_{NO,in}\\ \delta T_{g,in}\\ \delta u_{in}\end{pmatrix}$$

and state variables up to the *i*'th segment instead of $\mathbf{u}_i$. For example, the second segment's state space equation is expressed as follows:

$$\begin{aligned}\dot{\mathbf{x}}_2 &= \mathbf{A}_2\mathbf{x}_2 + \mathbf{B}_2\mathbf{y}_1 = \mathbf{A}_2\mathbf{x}_2 + \mathbf{B}_2(\mathbf{C}_1\mathbf{x}_1 + \mathbf{D}_1\mathbf{u})\\ &= \mathbf{B}_2\mathbf{C}_1\mathbf{x}_1 + \mathbf{A}_2\mathbf{x}_2 + \mathbf{B}_2\mathbf{D}_1\mathbf{u}\end{aligned} \tag{44}$$

The output matrix of the second segment can be also expressed by system input and state variables as follows:

$$\begin{aligned}\mathbf{y}_2 &= \mathbf{C}_2\mathbf{x}_2 + \mathbf{D}_2\mathbf{y}_1 = \mathbf{C}_2\mathbf{x}_2 + \mathbf{D}_2\left(\mathbf{C}_1\mathbf{x}_1 + \mathbf{D}_1\mathbf{u}\right) \\ &= \mathbf{D}_2\mathbf{C}_1\mathbf{x}_1 + \mathbf{C}_2\mathbf{x}_2 + \mathbf{D}_2\mathbf{D}_1\mathbf{u}\end{aligned} \tag{45}$$

Equation (46) summarizes (37) and (42) into one large state space equation that includes 15 state space equations for 15 segments.

$$\frac{d}{dt}\begin{pmatrix}\mathbf{x}_1\\ \mathbf{x}_2\\ \mathbf{x}_3\\ \mathbf{x}_4\\ \mathbf{x}_5\\ \cdot\\ \mathbf{x}_{12}\\ \mathbf{x}_{13}\\ \mathbf{x}_{14}\\ \mathbf{x}_{15}\end{pmatrix} = \begin{pmatrix} \mathbf{A}_1 & & & & & & & & & & & & \\ \mathbf{B}_2\mathbf{C}_1 & \mathbf{A}_2 & & & & & & & & & & & \\ \mathbf{B}_3\mathbf{D}_2\mathbf{C}_1 & \mathbf{B}_3\mathbf{C}_2 & \mathbf{A}_3 & & & & & & & & & & \\ \mathbf{B}_4\mathbf{D}_3\mathbf{D}_2\mathbf{C}_1 & \mathbf{B}_4\mathbf{D}_3\mathbf{C}_2 & \mathbf{B}_4\mathbf{C}_3 & \mathbf{A}_4 & & & & & & & & & \\ \mathbf{B}_5\mathbf{D}_4\mathbf{D}_3\mathbf{D}_2\mathbf{C}_1 & \mathbf{B}_5\mathbf{D}_4\mathbf{D}_3\mathbf{C}_2 & \mathbf{B}_5\mathbf{D}_4\mathbf{C} & \mathbf{B}_5\mathbf{C}_4 & \mathbf{A}_5 & & & & & & & & \\ \cdot & \cdot & \cdot & \cdot & \cdot & \cdot & & & & & & & \\ \cdot & \cdot & \cdot & \cdot & \cdot & \cdot & \mathbf{A}_{12} & & & & & & \\ \cdot & \cdot & \cdot & \cdot & \cdot & \cdot & \mathbf{B}_{13}\mathbf{C}_{12} & \mathbf{A}_{13} & & & & & \\ \cdot & \cdot & \cdot & \cdot & \cdot & \cdot & \mathbf{B}_{14}\mathbf{D}_{13}\mathbf{C}_{12} & \mathbf{B}_{14}\mathbf{C}_8 & \mathbf{A}_{14} & & & & \\ \mathbf{B}_{15}\mathbf{D}_{14}\mathbf{D}_{13}\cdots\mathbf{D}_2\mathbf{C}_1 & \cdot & \cdot & \cdot & \cdot & \cdot & \mathbf{B}_{15}\mathbf{D}_{14}\mathbf{D}_{13}\mathbf{C}_{12} & \mathbf{B}_{15}\mathbf{D}_{14}\mathbf{C}_{13} & \mathbf{B}_{15}\mathbf{C}_{14} & \mathbf{A}_{15} & & & \end{pmatrix}\begin{pmatrix}\mathbf{x}_1\\ \mathbf{x}_2\\ \mathbf{x}_3\\ \mathbf{x}_4\\ \mathbf{x}_5\\ \cdot\\ \mathbf{x}_{12}\\ \mathbf{x}_{13}\\ \mathbf{x}_{14}\\ \mathbf{x}_{15}\end{pmatrix} + \begin{pmatrix}\mathbf{B}_1\\ \mathbf{B}_2\mathbf{D}_1\\ \mathbf{B}_3\mathbf{D}_2\mathbf{D}_1\\ \mathbf{B}_4\mathbf{D}_3\mathbf{D}_2\mathbf{D}_1\\ \mathbf{B}_5\mathbf{D}_4\mathbf{D}_3\mathbf{D}_2\mathbf{D}_1\\ \cdot\\ \cdot\\ \cdot\\ \cdot\\ \mathbf{B}_{15}\mathbf{D}_{14}\mathbf{D}_{13}\cdots\mathbf{D}_2\mathbf{D}_1\end{pmatrix}\cdot\mathbf{u} \tag{46}$$

and output equation is as follows:

$$\mathbf{y} = \begin{pmatrix}\mathbf{D}_{15}\mathbf{D}_{14}\mathbf{D}_{13}\cdots\mathbf{D}_2\mathbf{C}_1 & \mathbf{D}_{15}\mathbf{D}_{14}\mathbf{D}_{13}\cdots\mathbf{D}_3\mathbf{C}_2 & \cdot & \cdot & \cdot & \mathbf{D}_{15}\mathbf{C}_{14} & \mathbf{C}_{15}\end{pmatrix}\cdot\begin{pmatrix}\mathbf{x}_1\\ \mathbf{x}_2\\ \mathbf{x}_3\\ \mathbf{x}_4\\ \mathbf{x}_5\\ \cdot\\ \mathbf{x}_{12}\\ \mathbf{x}_{13}\\ \mathbf{x}_{14}\\ \mathbf{x}_{15}\end{pmatrix} + \mathbf{D}_{14}\mathbf{D}_{13}\cdots\mathbf{D}_2\mathbf{D}_1\cdot\mathbf{u} \tag{47}$$

where, $\mathbf{x}_i = \begin{pmatrix}\delta\theta_i\\ \delta T_{w,i}\end{pmatrix}$, $\mathbf{y} = \begin{pmatrix}\delta C_{NH_3,out}\\ \delta C_{NO,out}\\ \delta T_{g,out}\end{pmatrix}$, and $\mathbf{u} = \begin{pmatrix}\delta C_{NH3,in}\\ \delta C_{NO,in}\\ \delta T_{g,in}\\ \delta u_{in}\end{pmatrix}$

VALIDATION

We evaluate the extent of accuracy of the linearized state-space model in Equation (46) by comparing its response to range of step inputs with those of the full-scale nonlinear model at different operating conditions. Table 2 and Figure 10 show the set of operating points considered. The gas temperature was fixed at 225 ^{o}C, and space velocity at 30,000 /Hr. Step inputs of 10 ppm in $\delta C_{NH_3,in}$ were introduced into the linear as well as nonlinear models. Figure 11 shows the resulting responses of $NH_{3,out}$, and, as expected, there is very little difference between the performances of the nonlinear and linear models for these inputs.

We also observed from our simulation studies that the range of inputs leading to accurate responses using linearized models was smaller in case 1 than those in cases 0 and 2. This is because the system dynamics changes very rapidly across the stoichiometric line which is spanned by case 1. We also found that the system dynamics is largely determined by the difference between the nominal Ammonia concentration and Nitrogen Monoxide concentration, making the normal to the stoichiometric line the dominant direction along which the system dynamics varies. This will be explained in the next section in detail.

Table 2 Nominal input conditions for the example of linearization simulations (T_w=225 °C, SV=30,000/Hr)

	$C_{NH_3,in}$ (ppm)	$C_{NO,in}$ (ppm)
Case #0	262.5	350
Case #1	350	350
Case #2	437.5	350

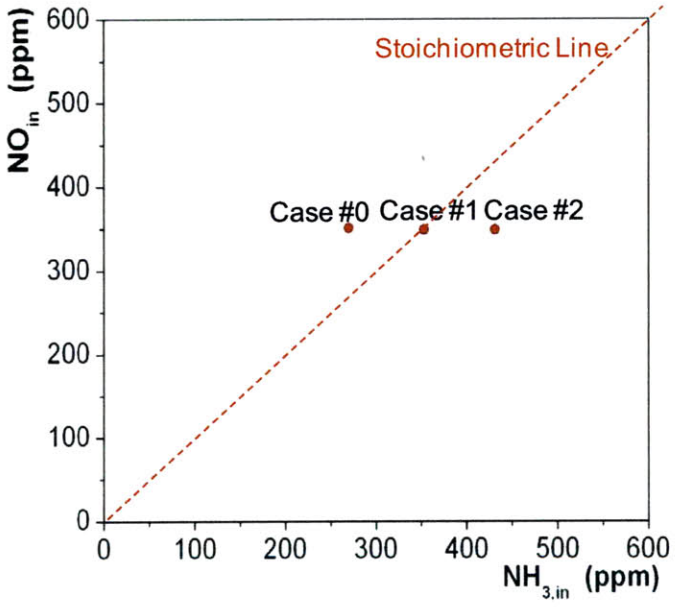

Figure 10 Nominal inputs for the simulations in the input map

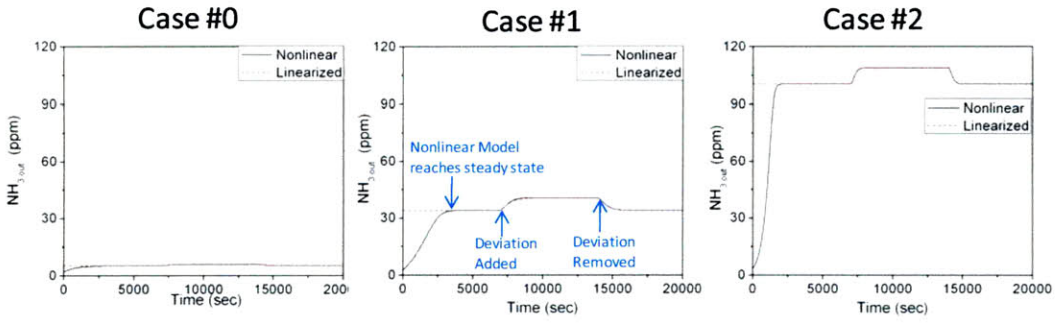

Figure 11 Comparison between linearized simulation and nonlinear simulation

SYSTEM DYNAMICS CHARCTERISTICS OF CATALYST

Given that the underlying SCR dynamics is nonlinear, a linearized approach implies that in order to truly capture all aspects of the SCR dynamics, a family of linearized models is required. The discussions in the previous section indicate that the linearized dynamics indeed varies as the operating point varies. Four nominal inputs such as Ammonia concentration, Nitrogen Monoxide concentration, gas temperature, and space velocity determine state variables of each segment under the equilibrium point. In this thesis, we do not consider the effect of space velocity variation, and we fixed the space velocity at 30,000 /Hr. In addition, we analyzed system dynamic variation according Ammonia and Nitrogen Monoxide concentration while keeping gas temperature fixed (e.g. T_g=225 °C). Because we assumed that there is no heat loss to ambient, the wall temperature T_w is the same as the Gas temperature T_g at the equilibrium. As the distance between the operating point and the stoichiometric line increases, the dynamics of the linearized model begins to vary. Therefore, we divide the operating points into three distinct regions, Regions 0, 1, and 2 (see Figure 12), which represent for insufficient Ammonia supply, stoichiometric Ammonia supply, and excess Ammonia supply condition, respectively. In other words, if excess Ammonia is supplied, the dynamics of the linearized model are similar at any point in Region 2, although there is a little variation according to nominal input condition. All of these in Region 2 are, however, quite different from when either insufficient or stoichiometric Ammonia is supplied. The reason for this difference may be explained as follows. In a standard SCR reaction (Equation (8)), the number of molecules of Ammonia is the same as that of Nitrogen Monoxide. Therefore, if excess Ammonia is supplied for long time and the system reaches equilibrium, the potential of Ammonia to be adsorbed onto the catalyst is less than the

case of stoichiometric supply of Ammonia, and as a result, adsorption reaction rates are less than in other cases. Similarly, if deficient Ammonia is supplied and the system reaches equilibrium, the adsorption rate is higher than both the cases of stoichiometric and excess supply of Ammonia, so adsorption rate is the highest among the three regions. This kinetic characteristic makes the system dynamics vary and can be broadly grouped into Regions 0, 1, and 2. This difference is also illustrated in Figure 13, which shows the frequency responses of each of the three regions.

We also observed dynamic patterns within each region. The system dynamics in Region 1 gets faster if the nominal input of NH_3 increases along the stoichiometric line. For example, the first-order model's pole location for 300 ppm concentration of $NH_{3,in}$ and NO_{in}, denoted as Position 1 in Figure 14, is 0.001066 rad/s and pole location for 400 ppm concentration of $NH_{3,in}$ and NO_{in}, denoted as Position 2 in Figure 14, is 0.001275 rad/s. This characteristic was observed in Regions 0 and 2 as well. This means that the system gets faster if the input concentration increases in the direction paralleling the stoichiometric line. However, the effect of variations in the direction normal to stoichiometric line was much higher than those in the parallel direction. For example, suppose that the input varies in Region 0 along line parallel and normal to stoichiometric line. The first order model's pole location for $(C_{NH3,in}, C_{NO,in})$ = (300 ppm, 300 ppm) , which is Position 1 in Figure 14, is 0.001066 rad/s, but the pole location for the input (200, 400), Position 3 in Figure 14, which is 200 ppm $NH_{3,in}$ and 400 ppm NO_{in} , is 0.003551 rad/s . In addition, pole location for the input (500, 300) Position 4 in Figure 14 is 0.003484, and pole location for the (600,800) is 0.003459 rad/s. In summary, for the same amount variation of length $100\sqrt{2}$ in the input map, change in a direction normal to the stoichiometric line changes the pole value by more than 35 times than that in the parallel

direction. Hence, it is reasonable to estimate the system dynamics of the catalyst in Region 0 and 2 by varying the input condition only along the normal to stoichiometric line, with the dynamics affected primarily by the perpendicular length from the line to nominal input condition. This characteristic is summarized in Figure 15 which shows the pole location variations both along a line parallel to and along a line normal to the stoichiometric line (top and bottom figures on the right side of Figure 15). It is easily discernable that the normal direction variation of inputs makes the system dynamic change a lot more.

The above discussions clearly indicate the entire family of linearized SCR dynamics can be represented by three linear models, denoted as Models 0, 1, and 2, that represent the dynamics in Regions 0, 1, and 2. And in Region 0 and 2, the details of the dynamics are determined by the distance of the nominal input position is away from the stoichiometric line in the normal direction, and, in Region 1, dynamics are determined by the length from the origin of the map.

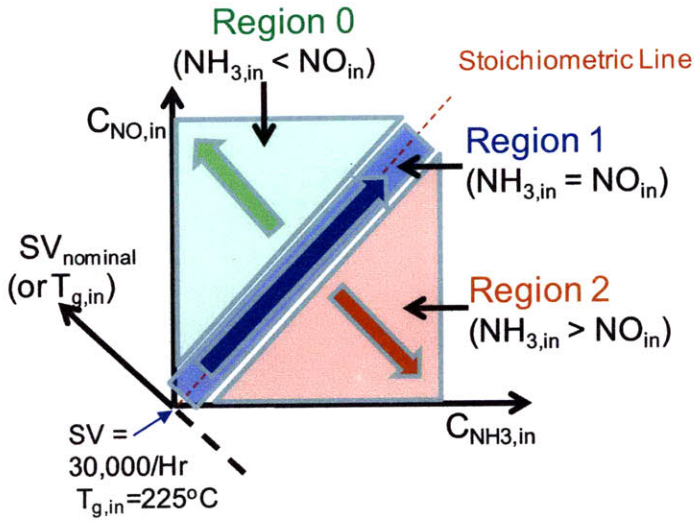

Figure 12 Nominal input map.

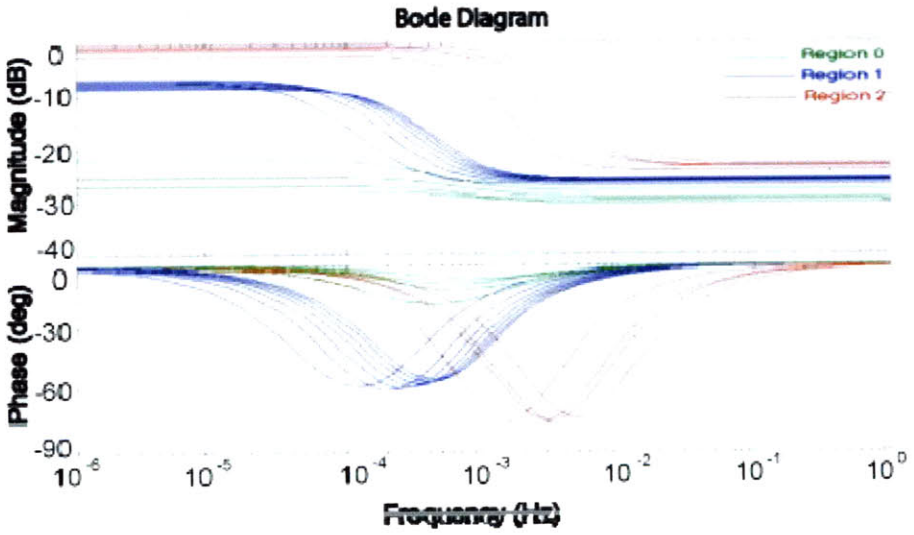

Figure 13 Comparison of frequency responses.

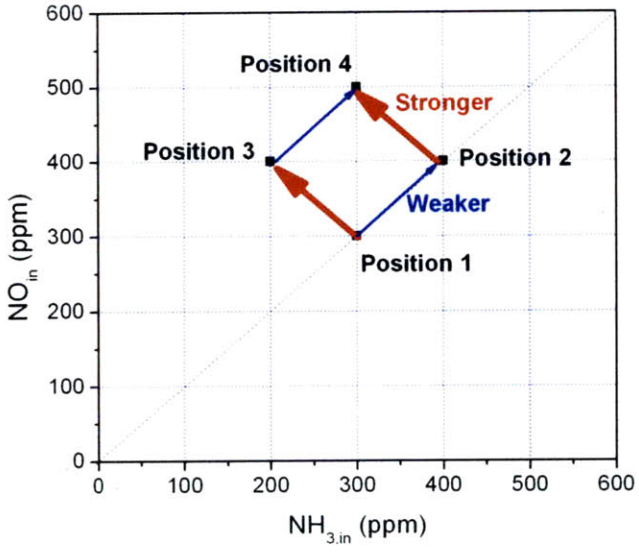

Figure 14 The effect of nominal input variation's direction

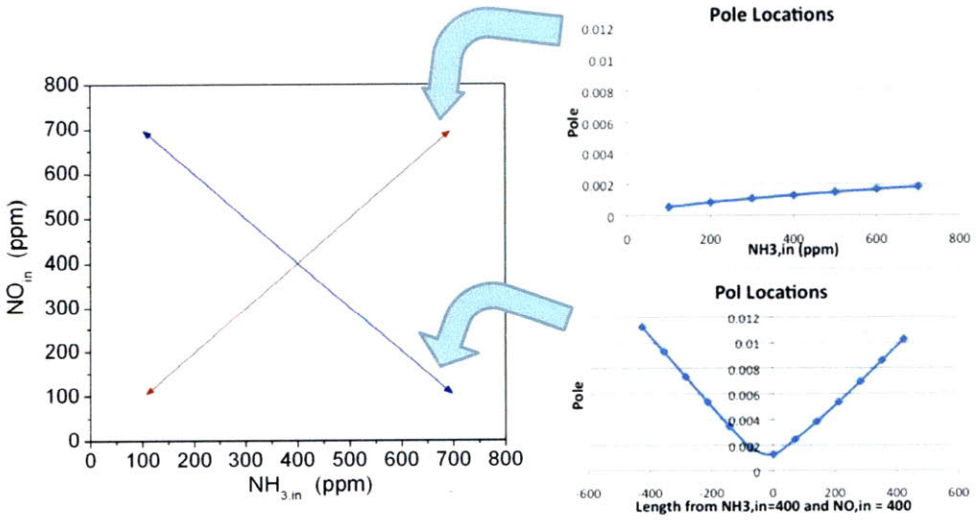

Figure 15 Pole location variations along the line parallel and normal to stoichiometric line

REDUCED ORDER MODEL

The discussions in the previous section allowed us to reduce the dynamics to that of three linear models representing Regions 0, 1, and 2. However, within each region, the underlying model is still complex since the system order is large and depends on the number of axial segments of discretization. We observed this number to be 30 (15 for θ_i and 15 for $T_{w,i}$) for an accurate model. As such, these models are not amenable for control due to the large computation burden they would entail. In addition, these models will include an equally large number of parameters and as such difficult to provide physical interpretation of the system dynamics. Therefore, in this section, we deploy model reduction methods to reduce the system order. While several model-reduction methods of internal balanced truncation, Balanced residualization, and Hankel norm minimization have been proposed in the literature [10], we focused on the internal balanced truncation method and is described below.

INTERNAL BALANCED TRUNCATION METHOD

In an internal balanced truncation method, the underlying system is first transformed to a balanced realization in which controllability and observability Grammians are equal and diagonal. A system represented state space form ($\mathbf{A,B,C,D}$) is said to be balanced if following Lyapunov equations are met [10].

$$\mathbf{AP} + \mathbf{PA}^{\mathrm{T}} + \mathbf{BB}^{\mathrm{T}} = 0 \tag{48}$$

$$\mathbf{A}^{\mathrm{T}}\mathbf{Q} + \mathbf{QA} + \mathbf{C}^{\mathrm{T}}\mathbf{C} = 0 \tag{49}$$

where, $\mathbf{P}$ and $\mathbf{Q}$ are controllability and observability Gramminians.

$\mathbf{A,B,C}$ matrices can be partitioned as follows:

$$\mathbf{A} = \begin{bmatrix} \mathbf{A}_{11} & \mathbf{A}_{12} \\ \mathbf{A}_{21} & \mathbf{A}_{22} \end{bmatrix} \quad \mathbf{B} = \begin{bmatrix} \mathbf{B}_1 \\ \mathbf{B}_2 \end{bmatrix} \quad \mathbf{C} = \begin{bmatrix} \mathbf{C}_1 & \mathbf{C}_2 \end{bmatrix} \tag{50}$$

Balanced truncation leads to a reduced order model described by ($\mathbf{A}_{11}, \mathbf{B}_1, \mathbf{C}_1, \mathbf{D}$) in which the states related to small Hankel singular values are discarded [10].

REDUCED ORDER MODEL RESULTS

The linearized model Equation (46) captures the effect of input deviation of Ammonia, Nitrogen Monoxide, gas temperature, and space velocity on the linearized system. Since the

control input into the system is Ammonia supply, the other inputs Nitrogen Monoxide, gas temperature, and velocity can be treated as disturbances as Figure 16. In this thesis, we focus our attention on system dynamics for the fixed gas temperatures and space velocity at 30,000/Hr. However, the results derived here can be extended to the case when these disturbances are not fixed. Therefore, for an input $\mathbf{u} = \left(\delta C_{NH3,in}\right)$ and disturbance $\delta C_{NO,in}$, the system matrix can be described as

$$\frac{d}{dt}\begin{pmatrix}\delta\theta_1\\ \delta\theta_2\\ \delta\theta_3\\ \delta\theta_4\\ \cdot\\ \cdot\\ \cdot\\ \cdot\\ \delta\theta_{14}\\ \delta\theta_{15}\end{pmatrix} = \begin{pmatrix} \mathbf{A}_1(1,1) & & & & & & & & & \\ \mathbf{B}_2\mathbf{C}_1(1,1) & \mathbf{A}_2(1,1) & & & & & & & & \\ \mathbf{B}_3\mathbf{D}_2\mathbf{C}_1(1,1) & \mathbf{B}_3\mathbf{C}_2(1,1) & \mathbf{A}_3(1,1) & & & & & & & \\ \mathbf{B}_4\mathbf{D}_3\mathbf{D}_2\mathbf{C}_1(1,1) & \mathbf{B}_4\mathbf{D}_3\mathbf{C}_2(1,1) & \mathbf{B}_4\mathbf{C}_3(1,1) & \mathbf{A}_4(1,1) & & & & & & \\ \cdot & \cdot & \cdot & \cdot & \cdot & & & & & \\ \cdot & \cdot & \cdot & \cdot & \cdot & \cdot & & & & \\ \cdot & \cdot & \cdot & \cdot & \cdot & \cdot & \cdot & & & \\ \cdot & \cdot & \cdot & \cdot & \cdot & \cdot & \cdot & \cdot & & \\ \cdot & \cdot & \cdot & \cdot & \cdot & \cdot & \cdot & \cdot & \mathbf{A}_{14}(1,1) & \\ \mathbf{B}_{15}\mathbf{D}_{14}\cdots\mathbf{D}_2\mathbf{C}_1(1,1) & \cdot & \cdot & \cdot & \cdot & \cdot & \cdot & \mathbf{B}_{15}\mathbf{C}_{14}(1,1) & \mathbf{A}_{15}(1,1) \end{pmatrix}\begin{pmatrix}\delta\theta_1\\ \delta\theta_2\\ \delta\theta_3\\ \delta\theta_4\\ \cdot\\ \cdot\\ \cdot\\ \cdot\\ \delta\theta_{14}\\ \delta\theta_{15}\end{pmatrix} + \begin{pmatrix} \mathbf{B}_1(1,1:2) \\ \mathbf{B}_2\mathbf{D}_1(1,1:2) \\ \mathbf{B}_3\mathbf{D}_2\mathbf{D}_1(1,1:2) \\ \mathbf{B}_4\mathbf{D}_3\mathbf{D}_2\mathbf{D}_1(1,1:2) \\ \cdot \\ \cdot \\ \cdot \\ \cdot \\ \cdot \\ \mathbf{B}_{15}\mathbf{D}_{14}\mathbf{D}_{13}\cdots\mathbf{D}_2\mathbf{D}_1(1,1:2) \end{pmatrix}\cdot\begin{pmatrix}\delta C_{NH3,in}\\ \delta C_{NO,in}\end{pmatrix} \tag{51}$$

where $\mathbf{A}_1(1,1)$ is the component of the first row and the first column, and $\mathbf{B}_1(1,1:2)$ means a sub matrix of the first row and the first and second column of $\mathbf{B}_1$.

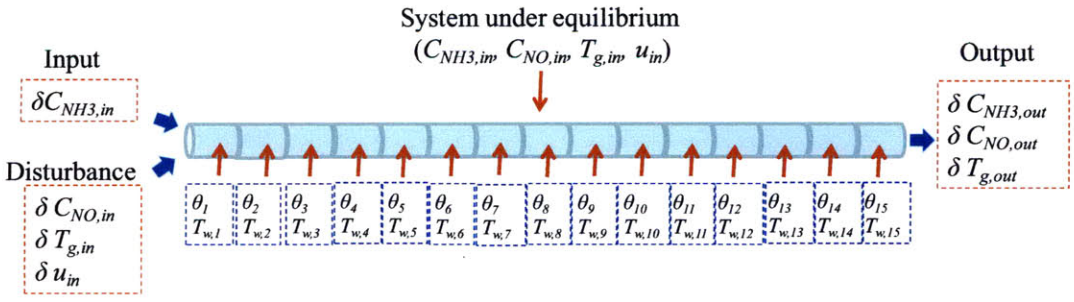

Figure 16 Input, disturbance, and outputs of the entire system

Looking at Figure 13 which shows frequency responses from $\delta C_{NH3,in}$ to $\delta C_{NH3,out}$, it was observed that the 30th order system could be reduced to at least a second order system with sufficiently high accuracy. For example, the transfer function between $\delta C_{NH_3,in}$ and $\delta C_{NH_3,out}$ can be reduced to the first order (Equation (52)) or the second order (Equation (53)) of Model 1, which belongs to Region 1, as follows:

$$G_{1,1} = \frac{k_{1,1}\left(s + z_{1,1}\right)}{\left(s + p_{1,1}\right)} \tag{52}$$

$$G_{1,1} = \frac{k_{1,1}\left(s^2 + c_1 \cdot s + d_1\right)}{\left(s^2 + a_1 \cdot s + b_1\right)} \tag{53}$$

These reductions were achieved using the internal balanced truncation method discussed above. Transfer functions relating $\delta C_{NH_3,in}$ to $\delta C_{NO,out}$ can be also reduced to the first order (Equation (54)) or the second order (Equation (55)) of Model 1 as follows:

$$G_{2,1} = \frac{k_{2,1}}{\left(s + p_{1,1}\right)} \tag{54}$$

$$G_{2,1} = \frac{k_{2,1}\left(s + e_1\right)}{\left(s^2 + a_1 \cdot s + b_1\right)} \tag{55}$$

where, the first subscript of $G_{1,1}$ of Equations (52) and (53) is an index relating input to output, and the second subscript is an index of model. For example, $G_{1,1}$ is the transfer function

relating $\delta NH_{3,in}$ to $\delta NH_{3,out}$ for Model 1 whose nominal input belongs to Region 1 in Figure 12, and $G_{2,0}$ is transfer function relating $\delta NH_{3,in}$ to δNO_{out} for Model 0 whose nominal input belongs to Region 0 in Figure 12. The parameters as $p_{1,1}$, $z_{1,1}$, $k_{1,1}$, and $k_{2,1}$ of the Model 1's first order model and the parameters as a_1, b_1, c_1, d_1, e_1, $k_{1,1}$, and $k_{2,1}$ of the Model 1's second order model are given in Appendix B for some nominal input conditions. The first and second order reduced model equation forms in Region 0 and Region 2 are also given in Appendix B, with their parameters at some nominal input conditions. For example, if 300 ppm Ammonia and Nitrogen Monoxide input are supplied, wall temperature is 225 °C, and space velocity is 30,000 /Hr, then $k_{1,1}$ = 0.01827, $z_{1,1}$=0.04197, and p_1=0.001066 for the first order model (Equation (52)) and $k_{1,1}$ =0.01827, a_1 =0.004931, $b_1 = 6.692\times10^{-6}$, c_1 =0.02449, d_1 =0.0002367 for the second order model (Equation(53)).

The error bound corresponding to the internal balanced truncation method is defined as follows [10]:

$$E^* = \left\| \mathbf{G} - \mathbf{G_R} \right\|_\infty \tag{56}$$

where, $\mathbf{G}$ and $\mathbf{G_R}$ are transfer functions of original system and reduced order model, respectively. The error bound of the first order model was found to be around 0.1353, and for the second order model is around 0.0027 for 300 ppm $C_{NH_3,in}$ and $C_{NO,in}$.

These reduced-order models are also compared via their step and frequency responses. A nominal operating condition is the same as before, and a step input of 5 ppm $\delta C_{NH_3,in}$ was supplied. The comparison of frequency response between the 30th order linearized system and the

reduced-order models in Equations (52) and (53) is shown in Figure 17. The step responses comparisons between the nonlinear model, 30^{th} order linearized model, and 1^{st} and 2^{nd} order models are also shown in Figure 18.

Equations (52), (53), and the responses shown in Figure 17 and Figure 18 imply that a first order model with four parameters or a second-order model with seven parameters is sufficient to describe the SCR response to changes in $\delta C_{NH_3,in}$, with the latter providing better accuracy. Therefore, as Figure 19, the original system whose system order is 30 can be reduced to the first or second reduced order system.

If the system is reduced to the first order, four parameters ($k_{1,k}$, $k_{2,k}$, $p_{1,k}$, and $z_{2,k}$) are needed for each model, which means that 3 set of the four parameters are need for Region 0, 1, and 2, are needed to know the effect of Ammonia input deviation ($\delta C_{NH_3,in}$) on the system. If the system is reduced to the second order, seven parameters ($k_{1,k}$, $k_{2,k}$, a_k, b_k, c_k, d_k and e_k) are needed for each model.

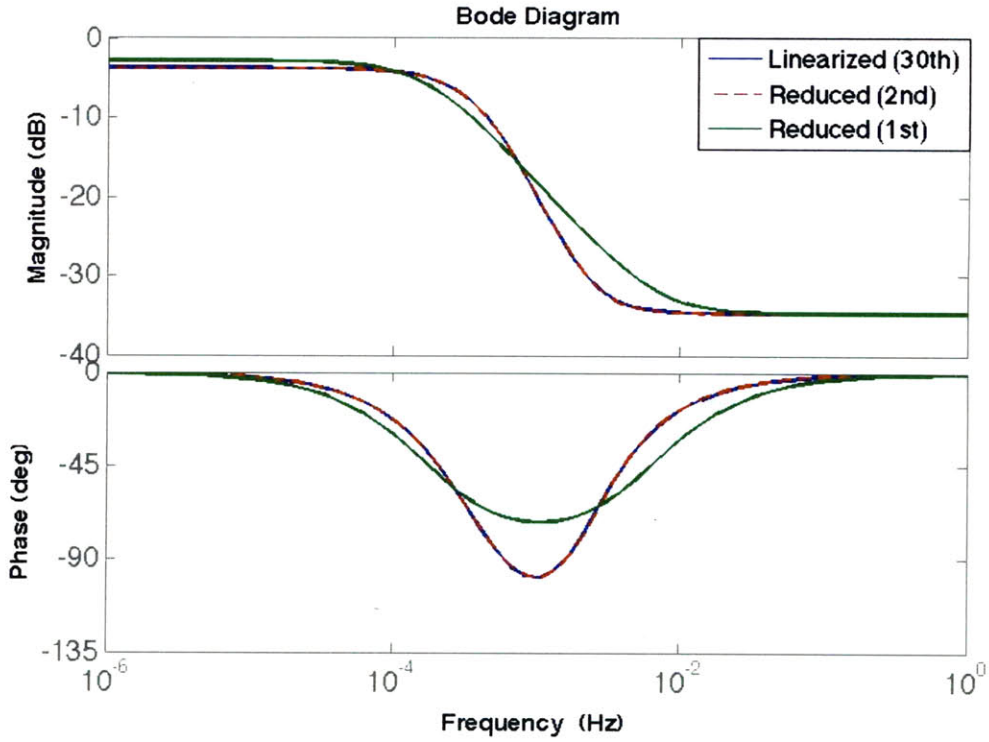

Figure 17 Comparison of frequency response among 30th order linearzied model, 1st and 2nd order reduced model.

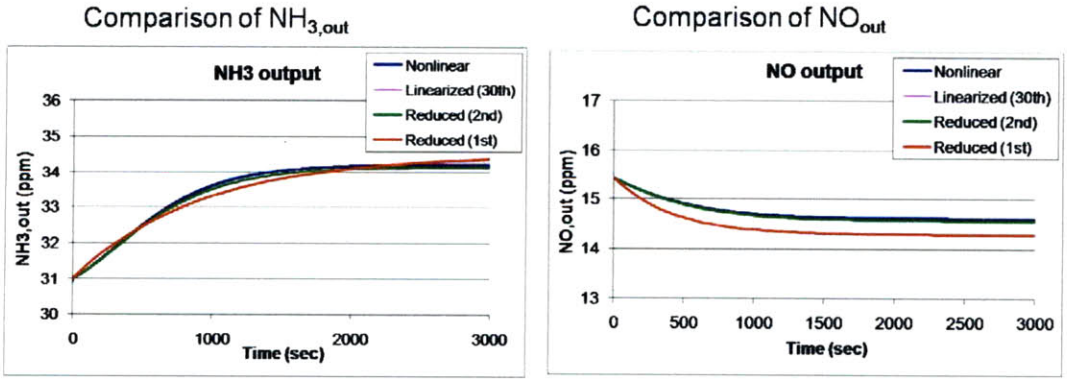

Figure 18 Comparison of step responses between nonlinear, 30th order linearized models, and reduced order models

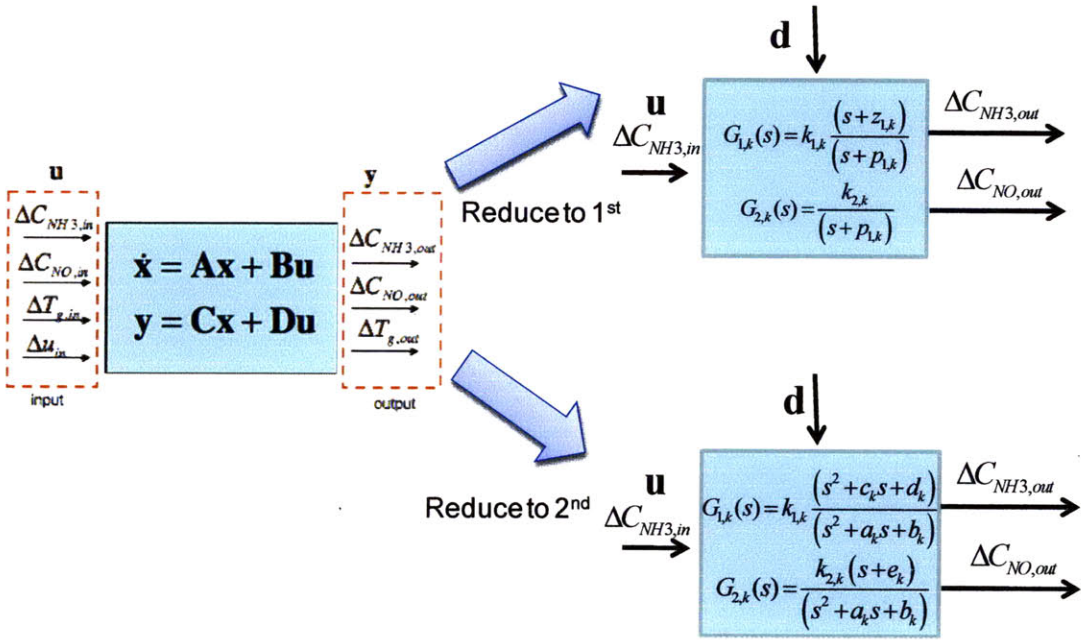

Figure 19 The first and second reduced order systems

PHYSICAL INTERPRETATIONS

The main contribution of this thesis is the development of a systematic methodology that yields a reduced-order model of the SCR dynamics starting from a first-principles model. The parameters of this model are related to the operating conditions in a transparent manner, and their variations captured. The next step in this modeling procedure is a physical interpretation for these variations. As the project concluded before carrying out this important step, these interpretations are not provided in this report, but a few observations are made.

The first observation is that the poles become faster if the nominal input condition increases in a direction parallel to the stoichiometric line (see Figure 15). This may be due to the fact that a higher concentration results in a higher value of θ, which in turn invokes higher reaction rates there by making the system dynamics faster. The second observation is that as the magnitude of the nominal input is away from the stoichiometric line, the system dynamics get faster in Region 0 and Region 2. And, the DC gain in Region 0 (and 2) decreases (and increases) as the nominal inputs move away from the stoichiometric line in the normal direction. The effect of the DC gain variation may be explained as follows. If the nominal input position moves away from the stoichiometric line by some amount in Region 0, then this means that the system is supplied less than sufficient Ammonia, which in turn causes the θ values to get lower. A lower $C_{NH_3,in}$ increases adsorption reaction rates, and hence the DC gain of $\delta C_{NH_3,in}$ to $\delta C_{NO,in}$ decreases. The explanation for an increasing pole-magnitude in Region 0 may be as follows. As the operating point move away from stoichiometric line in Region 1, the Ammonia input decreases compared to NO_x. As a result, θ at equilibrium decreases. This in turn causes the system to respond rapidly to io incoming $NH_{3,in}$ and causes the pole to become faster. A similar

explanation can be given for the dynamics variation in Region 2.

Another interesting observation is that the reduced-order of the underlying model is at most two. It is not clear if specific physical meaning can be attached to these two states. The underlying model-reduction method employed, internal balance reduction, essentially transforms the system coordinates to a balanced form, which rearranges the state variables in the order of their singular values. Therefore, the two state variables in the second order reduced system are essentially related to the two dominant time-constants of the system. A more explicit physical meaning of these time-constants is yet to be determined.

An additional point to be noted is regarding the spatial discretizations. From nonlinear simulations, we found that the initial segments play a more important role in reducing Nitrogen Monoxide, because their stored Ammonia values are higher than those of rear segments. The reduction rates of Nitrogen Monoxide in these segments are higher, since the chemical reaction rates in the catalyst is strongly dependent on Ammonia fraction θ as shown in Equations (10) to (13). In the first order dynamic model, these dependencies are lumped into one parameter, making any correlation between time-constants and specific spatial segments infeasible. In a second-order model, the balanced method reduction introduces two state values which may be related to Ammonia fractions θ corresponding broadly to two segments with one representing the early segments whose Ammonia fractions θ is high and the other representing the effect of later segments whose θ is small. This is indeed a topic for future work.

CORRELATIONS BETWEEN PARAMETERS AND INPUT CONDITIONS

One of the major advantages of a first-principles model is its tangibility. The parameters of the model can be determined using the physical and chemical constants of the underlying system, and as such, changes in the system dynamics with changes in the system as well as environmental conditions can be captured in a transparent manner. In the case of the SCR dynamics, the system dynamics changes with concentrations of $NH_{3,in}$, NO_{in}, $T_{g,in}$, and u_{in}. We evaluate these changes and attempt to model the corresponding changes in the reduced-order models derived above.

For example, our specific focus is on the model given by Equation (52), which is the first order model in Region 1, and its parameter variations with nominal input $C_{NH_3,in}$. Variations in the pole and zero values for six input conditions in Region 1 are shown in Figure 20. Using a curve-fit, these variations of pole, zero, and DC gain for the first order model are captured as Equations (57), (58), (59), and (60).

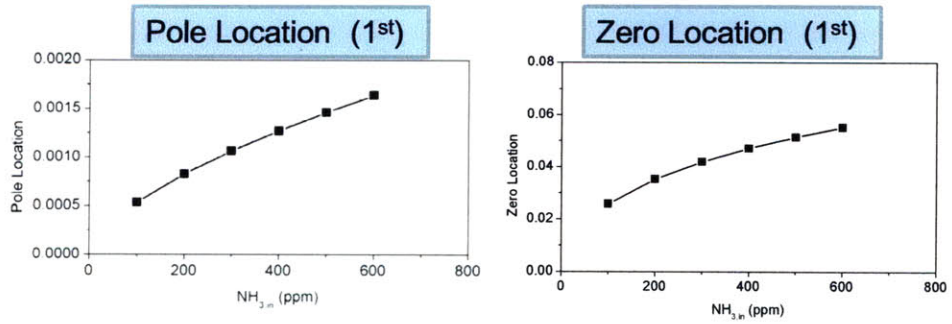

Figure 20 Pole and zero locations variation in Region 1.

$$p_{1,1} = -1.151\times10^{-9} C_{NH_3,in}^2 + 3.019\times10^{-6} C_{NH_3,in} + 2.548\times10^{-4} \quad (57)$$

$$z_{1,1} = -5.558\times10^{-8} C_{NH_3,in}^2 + 9.767\times10^{-5} C_{NH_3,in} + 1.721\times10^{-2} \quad (58)$$

$$k_{1,1} = -8.493\times10^{-9} C_{NH_3,in}^2 + 1.193\times10^{-5} C_{NH_3,in} + 1.537\times10^{-2} \quad (59)$$

$$k_{2,1} = 1.039\times10^{-9} C_{NH_3,in}^2 - 1.974\times10^{-6} C_{NH_3,in} - 1.941\times10^{-4} \quad (60)$$

A similar procedure is carried out for the models in Regions 0 and 2, where the variation in model parameters is determined as a function of DS, the distance of the input condition from the stoichiometric line, the most dominant parameter. These variations are captured in a curve-fit relation similar to Equation (57) to (60) in Appendix C. These relations allow the prediction of SCR dynamics at arbitrary nominal input conditions. For example, if the nominal input of Ammonia and Nitrogen Monoxide is 333 ppm, and wall temperature and space velocity is fixed at 498 K and 30,000 /Hr, then the parameters for the first order models can be obtained directly from Equations (57) to (60). $p_{1,1}$, $z_{1,1}$, $k_{1,1}$, and $k_{2,1}$ value for the input condition are 0.0011325, 0.043571, 0.018401, and -7.3623×10^{-4}, respectively.

SUMMARY OF THE MODELING PROCEDURE

In this section, the overall procedure for getting reduced order models is outlined.

1. Start with the nominal condition determined by $NH_{3,in}$, $NO_{x,in}$, $T_{g,in}$, and u_{in}.
2. Determine the region of the input condition as Region 0, 1, or 2, and use the corresponding Model 0, 1, or 2, using Figure 21. If the nominal input condition is located on the red dot in Figure 21, then this belongs to Region 1, and therefore Model 1 should be used.
3. Obtain parameters numerical values from the curve-fit relations from Appendix C. If a transfer function relating $\delta C_{NH3,in}$ to $\delta C_{NH3,out}$ is of interest and the second order model is chosen, then Equation (53) is used to predict the system dynamics under the input condition, and parameters ($k_{1,1}$, a_1, b_1, c_1, and d_1) of the transfer function are obtained from correlations from Equation (103), (105), (106), (107), and (108) in Appendix C. Figure 22 shows the accuracy of the model thus determined, for an input condition of $C_{NH_3,in} = C_{NO,in}$=333 ppm, $T_{g,in}$ =225 °C, and 30,000 /Hr space velocity.
4. If the nominal input condition changes to new values, repeat steps 1 to 3. Figure 23 is a comparison between nonlinear result and reduced order model result for a new nominal input condition of $C_{NH_3,in} = C_{NO,in}$=388 ppm, which shows that the corresponding linear model accurately predict the systems at the new input condition.

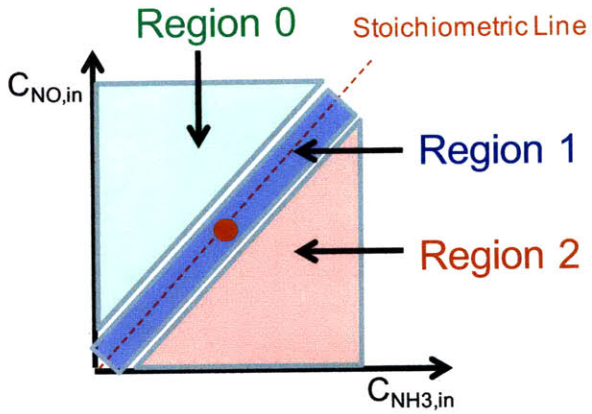

Figure 21 Step 2: choose region and select model

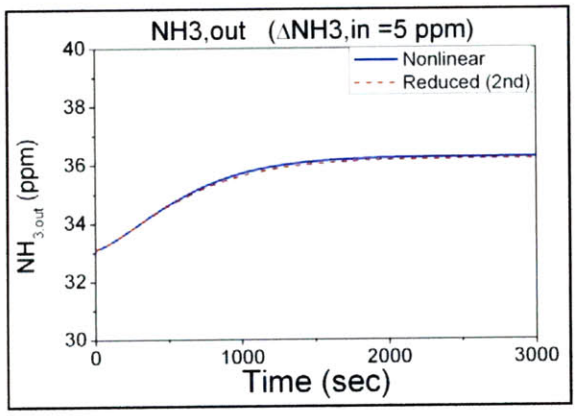

Figure 22 Step 3: 2nd reduced model describes the system dynamic accurately at input concentration of 333 ppm NH_3 and NO

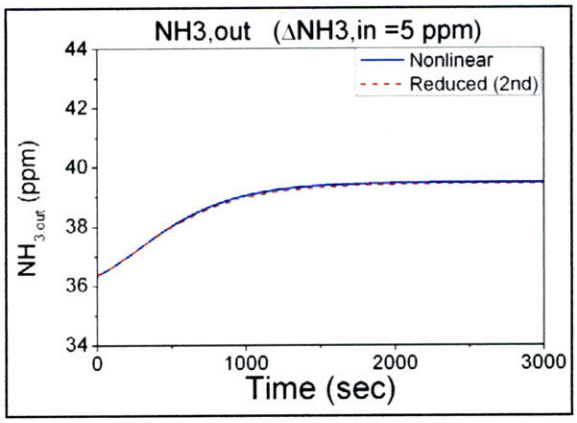

Figure 23 The new transfer function for the input concentration of 388 ppm NH_3 and NO also describes the system dynamics accuartely

SUMMARY AND CONCLUDING REMARKS

In this thesis, we first derived nonlinear models based on physical and chemical interpretation of the catalyst and certain simplifications. We subsequently discretized and linearized the nonlinear equations and analyzed the system dynamics of the catalyst. Finally, we reduced the system order. The following are some of our main observations regarding the SCR dynamic model.

1) The system dynamics of the catalyst can be grouped into three regions according to input conditions.
2) Three linear models can be introduced to represent Regions 0, 1, and 2, and in each model, there is dynamic variation.
3) System dynamic patterns exist. For example, the system gets faster in Region 1 as the input-concentrations increase, and the system gets faster in Region 0 and 2 as the nominal input is away from the stoichiometric line. Also, the DC gain in Region 0 (or 2) decreases (or increase) as the nominal input moves away from the stoichiometric line.
4) A second order reduced model, represented by the seven parameters can accurately describe the system dynamics.
5) In each region, the physical dependencies of the parameters on dominant operating conditions can be determined.

The above properties can be directly used to derive a systematic model-based advanced control design that allows a high NO_x conversion efficiency at minimum $NH_{3,slip}$.

REFERENCES

[1] Wikipedia, "Air pollution." vol. 2010, 2010.

[2] EPA, "Regulatory Announcement," PA420-F-00-057, Dec. 2000.

[3] Wikipedia, "Catalytic converter." vol. 2010, 2010.

[4] C. Y. Ong, "Adaptive PI Control of NOx Emissions in a Urea Selective Catalytic Reduction System using System Identification Models," in *Department of Mechanical Engineering*. vol. S.M. thesis Cambridge: Massachusetts Institute of Technology, 2010.

[5] J. Y. Kim, G. Cavataio, J. E. Patterson, P. M. Laing, and C. K. Lambert, "Laboratory Studies and Mathematical Modeling of Urea SCR Catalyst Performance," 2007.

[6] D. Upadhyay and M. Van Nieuwstadt, "Model based analysis and control design of a urea-SCR deNOx aftertreatment system," *Journal of Dynamic Systems Measurement and Control,* vol. 128, pp. 737-741, Sep 2006.

[7] D. Upadhyay and M. Van Nieuwstadt, "Modeling of a Urea SCR Catalyst with Automotive Applications," 2002.

[8] J. N. Chi and H. F. M. DaCosta, "Modeling and Control of a Urea-SCR Aftertreatment System," 2005.

[9] L. Lietti, I. Nova, S. Camurri, E. Tronconi, and P. Forzatti, "Dynamics of the SCR-DeNO(x) reaction by the transient-response method," *Aiche Journal,* vol. 43, pp. 2559-2570, Oct 1997.

[10] S. Skogestad and I. Postlethwaite, *Multivariable feedback control : analysis and design*, 2nd ed. Chichester, England ; Hoboken, NJ: John Wiley, 2005.

DEFINITIONS/ABBREVIATIONS

A nomenclature given by:

A	Cross section area $\left[m^2\right]$
C	Concentration of each species $\left[\frac{mol}{m^3}\right]$
C_p	Specific heat capacity $\left[\frac{KJ}{Kg \cdot K}\right]$
D	Mass transfer coefficient $\left[\frac{m}{s}\right]$
(g)	Gas-phase molecules
ΔH	Enthalpy of reaction $\left[\frac{KJ}{Mol}\right]$
h	Heat transfer coefficient
l	Perpendicular length from stoichiometric line
P	Perimeter $[m]$
p	Pre-exponential parameter
R	Reaction rate per reaction-sites $\left[\frac{mol}{s \cdot mole - sites}\right]$
R_u	Universal gas constant: 8.314 $\frac{J}{mol \cdot K}$
(s)	Adsorbed molecules
s	Number of reaction-sites per length (in governing equations)
s	Laplace variable (in transfer functions)
T	Temperature $[K]$
t	Time $[s]$
u	Gas velocity $\left[\frac{m}{s}\right]$
α	Parameter for the surface coverage dependency
ρ	Density $\left[\frac{kg}{m^3}\right]$
θ	Fractional NH_3 loading
Ω	Number of reaction-sites per washcoat volume

The subscripts used above denote the following:

a	Adsorption reaction
amb	Ambient
d	Desorption reaction
ex	Experimental data

g	Gas phase
i	Index of species
in	Values at inlet
j	Index of chemical reaction pathways
o	Oxidation reaction
out	Values at exit
r	Reduction reaction
s	Catalyst surface
sat	Saturated status data
sim	Simulation data
w	Wall
wt	Washcoat

Abbreviation

DS	Distance from stoichiometric line
PDE	Partial Differential Equation
SCR	Selective Catalytic Reduction
SV	Space Velocity

APPENDIX A

$$J_{11,i} = -p_a C_{NH_3,i,eq} - p_d \exp\left(-\frac{E_{d0}\left(1-\alpha\theta_{i,eq}\right)}{R_u \cdot T_{w,i,eq}}\right) - p_d \theta_{i,eq} \exp\left(-\frac{E_{d0}\left(1-\alpha\theta_{i,eq}\right)}{R_u \cdot T_{w,i,eq}}\right)\frac{\alpha E_{d0}}{R_u \cdot T_{w,i,eq}}$$
$$- p_r \exp\left(-\frac{E_r}{R_u \cdot T_{w,i,eq}}\right) C_{NO,i,eq} - p_o \exp\left(-\frac{E_o}{R_u \cdot T_{w,i,eq}}\right) C_{O_2} \tag{61}$$

$$J_{12,i} = -p_d \exp\left(-\frac{E_{d0}\left(1-\alpha\theta_{i,eq}\right)}{R_u \cdot T_{w,i}}\right)\theta_{eq} \cdot \frac{E_{d0}\left(1-\alpha\theta_{i,eq}\right)}{R_u \cdot T_{w,i}^2}$$
$$- p_r \exp\left(-\frac{E_r}{R_u \cdot T_{w,i}}\right)\theta_{eq} C_{NO,i,eq} \frac{E_r}{R_u \cdot T_{w,i}^2} - p_o \exp\left(-\frac{E_o}{R_u \cdot T_{w,i}}\right)\theta_{eq} C_{O_2} \frac{E_o}{R_u \cdot T_{w,i}^2} \tag{62}$$

$$J_{13,i} = p_a\left(1-\theta_{i,eq}\right) \tag{63}$$

$$J_{14,i} = -p_r \exp\left(-\frac{E_r}{R_u \cdot T_{w,i,eq}}\right)\theta_{eq} \tag{64}$$

$$J_{22} = -\frac{h \cdot P}{\rho_w A_w C_{P,w}} \tag{65}$$

$$J_{25,i} = \frac{h \cdot P}{\rho_w A_w C_{P,w}} \tag{66}$$

$$J_{31,i} = \frac{A_g u \cdot s \cdot \Delta x \cdot p_a \cdot C_{NH_3,i,eq}}{\left(A_g u + s\Delta x \cdot p_a \cdot (1-\theta_{i,eq})\right)^2} + \frac{\left(s \cdot \Delta x \cdot p_d\right)^2}{\left(A_g u + s\Delta x \cdot p_a \cdot (1-\theta_{i,eq})\right)^2} \exp\left(\frac{-E_{d0}(1-\alpha\theta_{i,eq})}{R_u \cdot T_{w,eq}}\right) \cdot \theta_{i,eq}$$
$$+ \frac{s \cdot \Delta x \cdot p_d}{A_g u + s\Delta x \cdot p_a \cdot (1-\theta_{i,eq})} \cdot \frac{E_{d0} \cdot \alpha}{R_u \cdot T_{w,eq}} \cdot \exp\left(\frac{-E_{d0}(1-\alpha\theta_{i,eq})}{R_u \cdot T_{w,eq}}\right) \cdot \theta_{i,eq} \tag{67}$$
$$+ \frac{s \cdot \Delta x \cdot p_d}{A_g u + s\Delta x \cdot p_a \cdot (1-\theta_{i,eq})} \exp\left(\frac{-E_{d0}(1-\alpha\theta_{i,eq})}{R_u \cdot T_{w,eq}}\right)$$

$$J_{32,i} = \frac{s \cdot \Delta x \cdot p_d}{A_g u + s\Delta x \cdot p_a \cdot (1-\theta_{i,eq})} \exp\left(\frac{-E_{d0}(1-\alpha\theta_{i,eq})}{R_u \cdot T_{w.i,eq}}\right) \cdot \theta_{i,eq} \cdot \frac{E_{d0} \cdot (1-\alpha\theta_{i,eq})}{\left(R_u \cdot T_{w,i,eq}\right)^2} \tag{68}$$

$$J_{33,i} = \frac{A_g u}{A_g u + s\Delta x \cdot p_a \cdot (1-\theta_{i,eq})} \tag{69}$$

$$J_{36,i} = \frac{A_g}{A_g u + s\Delta x \cdot p_a \cdot (1-\theta_{i,eq})} C_{NH3,i} + \frac{-A_g \cdot s \cdot \Delta x \cdot p_d}{\left(A_g u + s\Delta x \cdot p_a \cdot (1-\theta_{i,eq})\right)^2} \exp\left(\frac{-E_{d0}(1-\alpha\theta_{i,eq})}{R_u \cdot T_{w,i,eq}}\right) \cdot \theta_{i,eq} \tag{70}$$

$$J_{41,i} = \frac{-A_g u \cdot s \cdot \Delta x \cdot p_r \cdot \exp\left(-\frac{E_r}{R_u \cdot T_{w,i,eq}}\right) \cdot C_{NO,i,eq}}{\left(A_g u + s \cdot \Delta x \cdot p_r \cdot \exp\left(-\frac{E_r}{R_u \cdot T_{w,i,eq}}\right) \cdot \theta_{i,eq}\right)^2} \tag{71}$$

$$J_{42,i} = \frac{-A_g u \cdot s \cdot \Delta x \cdot p_r \cdot \exp\left(-\frac{E_r}{R_u \cdot T_{w,i,eq}}\right) \cdot \frac{E_r R}{\left(R_u \cdot T_{w,i,eq}\right)^2} \cdot C_{NO,i,eq} \cdot \theta_{i,eq}}{\left(A_g u + s \cdot \Delta x \cdot p_r \cdot \exp\left(-\frac{E_r}{R_u \cdot T_{w,i,eq}}\right) \cdot \theta_{i,eq}\right)^2} \tag{72}$$

$$J_{44,i} = \frac{A_g u}{A_g u + s \cdot \Delta x \cdot p_r \cdot \exp\left(-\frac{E_r}{R_u \cdot T_{w,i,eq}}\right) \cdot \theta_{i,eq}} \tag{73}$$

$$J_{46,i} = \frac{A_g}{A_g u + s \cdot \Delta x \cdot p_r \cdot \exp\left(-\frac{E_r}{R_u \cdot T_{w,i}}\right) \cdot \theta_i} C_{NO,i} + \frac{-A_g^2 u}{\left(A_g u + s \cdot \Delta x \cdot p_r \cdot \exp\left(-\frac{E_r}{R_u \cdot T_{w,i}}\right) \cdot \theta_i\right)^2} C_{NO,i} \tag{74}$$

$$J_{52,i} = \frac{h \cdot P \cdot \Delta x}{\rho_g A_g C_{p,g} u + h \cdot P \cdot \Delta x} \tag{75}$$

$$J_{55,i} = \frac{\rho_g A_g C_{p,g} u}{\rho_g A_g C_{p,g} u + h \cdot P \cdot \Delta x} \tag{76}$$

$$J_{56,i} = \left[\frac{u}{\rho_g A_g C_{p,g} u + h \cdot P \cdot \Delta x} + \frac{-\left(\rho_g A_g C_{p,g}\right)^2 u}{\left(\rho_g A_g C_{p,g} u + h \cdot P \cdot \Delta x\right)^2} \right] \cdot T_{g,i,eq} + \frac{-h \cdot P \cdot \rho_g A_g C_{p,g} \cdot \Delta x}{\left(\rho_g A_g C_{p,g} u + h \cdot P \cdot \Delta x\right)^2} \cdot T_{w,i,eq} \tag{77}$$

$$J_{66,i} = 1 \tag{78}$$

APPENDIX B

Nominal temperature in all data of Appendix B is 498 K

- The first order reduced model in Region 1.

Equation (79) is a transfer function relating $\delta C_{NH_3,in}$ to $\delta C_{NH_3,out}$, and Equation (80) is a transfer function relating $\delta C_{NH_3,in}$ to $\delta C_{NO,out}$.

$$G_{1,1} = \frac{k_{1,1}\left(s + z_{1,1}\right)}{\left(s + p_{1,1}\right)} \tag{79}$$

$$G_{2,1} = \frac{k_{2,1}}{\left(s + p_{1,1}\right)} \tag{80}$$

Table 3 Parameters of Equations (79) and (80)

$NH_{3,in}(=NO_{in})$ (ppm)	$k_{1,1}$	$z_{1,1}$	$p_{1,1}$	$k_{2,1}$
100	0.01636	0.02579	0.0005335	-0.00037066
200	0.017571	0.0353	0.0008266	-0.00055974
300	0.01827	0.04197	0.001066	-0.00070046
400	0.018753	0.04723	0.001275	-0.00081489
500	0.019119	0.05162	0.001467	-0.00091235
600	0.019409	0.05543	0.001645	-0.00099783
700	0.019649	0.05881	0.001813	-0.0010744

- The second order reduced model, Region 1.

Equation (79) is a transfer function relating $\delta C_{NH_3,in}$ to $\delta C_{NH_3,out}$, and Equation (80) is a transfer function relating $\delta C_{NH_3,in}$ to $\delta C_{NO,out}$.

$$G_{1,1} = \frac{k_{1,1}\left(s^2 + c_1 s + d_1\right)}{\left(s^2 + a_1 s + b_1\right)} \tag{81}$$

$$G_{2,1} = \frac{k_{2,1}\left(s + e_1\right)}{\left(s^2 + a_1 s + b_1\right)} \tag{82}$$

Table 4 Parameters of Equations (81) and (82)

$NH_{3,in}(=NO_{in})$ (ppm)	$k_{1,1}$	a_1	b_1	c_1	d_1	e_1	$k_{2,1}$
100	0.01636	0.002433	1.729E-06	0.01329	7.43E-05	0.005208	-0.00019994
200	0.017571	0.003806	4.084E-06	0.01967	0.0001559	0.008117	-0.00029926
300	0.01827	0.004931	6.692E-06	0.02449	0.0002369	0.01039	-0.00037542
400	0.018753	0.005923	9.471E-06	0.02849	0.0003168	0.0123	-0.00043896
500	0.019119	0.006829	1.238E-05	0.03197	0.0003954	0.01399	-0.00049429
600	0.019409	0.007673	1.541E-05	0.03508	0.0004732	0.01552	-0.00054376
700	0.019649	0.008472	1.855E-05	0.03792	0.0005502	0.01693	-0.00058883

- The first order reduced model, Region 0.

Equation (83) is a transfer function relating $\delta C_{NH_3,in}$ to $\delta C_{NH_3,out}$, and Equation (84) is a transfer function relating $\delta C_{NH_3,in}$ to $\delta C_{NO,out}$.

$$G_{1,0} = \frac{k_{1,0}\left(s + z_{1,0}\right)}{\left(s + p_{1,0}\right)} \tag{83}$$

$$G_{2,0} = \frac{k_{2,0}}{\left(s + p_{1,0}\right)} \tag{84}$$

Table 5 Parameters of Equations (83) and (84)

Length*	$k_{1,0}$	$z_{1,0}$	$p_{1,0}$	$k_{2,0}$
$50\sqrt{2}$	0.013517	0.01051	0.001754	-9.22E-05
$100\sqrt{2}$	0.011182	0.007633	0.003484	-2.79E-05
$150\sqrt{2}$	0.010101	0.008112	0.005389	-1.25E-05
$200\sqrt{2}$	0.0094602	0.009268	0.007332	-6.10E-06
$250\sqrt{2}$	0.0090296	0.01068	0.009296	-2.89E-06
$300\sqrt{2}$	0.0087185	0.01222	0.01127	-1.18E-06

* Length is the perpendicular length from stoichiometric line to nominal input

- The second order reduced model, Region 0.

Equation (79) is a transfer function relating $\delta C_{NH_3,in}$ to $\delta C_{NH_3,out}$, and Equation (80) is a transfer function relating $\delta C_{NH_3,in}$ to $\delta C_{NO,out}$.

$$G_{1,0} = \frac{k_{1,0}(s+c_0)(s+d_0)}{(s^2 + a_0 s + b_0)} \tag{85}$$

$$G_{2,0} = \frac{k_{2,0}(s+e_0)}{(s^2 + a_0 s + b_0)} \tag{86}$$

Table 6 Parameters of Equations (85) and (86)

Length*	$k_{1,0}$	a_0	b_0	c_0	d_0	e_0	$k_{2,0}$
$50\sqrt{2}$	0.013517	0.00569	0.001599	0.01023	0.005516	0.005602	-8.940E-05
$100\sqrt{2}$	0.011182	0.007449	0.003179	0.009443	0.005509	6.58E-03	-2.898E-05
$150\sqrt{2}$	0.010101	0.009061	0.005008	0.009911	0.006911	0.008408	-1.265E-05
$200\sqrt{2}$	0.0094602	0.01049	0.00694	0.01081	0.008537	0.008537	-6.054E-06
$250\sqrt{2}$	0.0090296	0.01180	0.008944	0.01184	0.01027	0.01176	-2.840E-06
$300\sqrt{2}$	0.0087185	0.01303	0.01100	0.01286	0.01210	0.0132	-1.155E-06

* Length is the perpendicular length from stoichiometric line to nominal input

- The first order reduced model, Region 2.

Equation (87) is a transfer function relating $\delta C_{NH_3,in}$ to $\delta C_{NH_3,out}$, and Equation (88) is a transfer function relating $\delta C_{NH_3,in}$ to $\delta C_{NO,out}$.

$$G_{1,2} = \frac{k_{1,2}\left(s + z_{1,2}\right)}{\left(s + p_{1,2}\right)} \tag{87}$$

$$G_{2,2} = \frac{k_{2,2}}{\left(s + p_{1,2}\right)} \tag{88}$$

Table 7 Parameters of Equations (87) and (88)

Length*	$k_{1,2}$	$z_{1,2}$	$p_{1,2}$	$k_{2,2}$
$50\sqrt{2}$	0.022726	0.1061	0.002442	-0.0023436
$100\sqrt{2}$	0.025472	0.163	0.003849	-0.0041244
$150\sqrt{2}$	0.027592	0.2185	0.005364	-0.0060795
$200\sqrt{2}$	0.029329	0.2728	0.006952	-0.0081654
$250\sqrt{2}$	0.030805	0.326	0.008593	-0.010351
$300\sqrt{2}$	0.032094	0.378	0.01027	-0.012615

* Length is the perpendicular length from stoichiometric line to nominal input

- The second order reduced model, Region 0.

Equation (89) is a transfer function relating $\delta C_{NH_3,in}$ to $\delta C_{NH_3,out}$, and Equation (90) is a transfer function relating $\delta C_{NH_3,in}$ to $\delta C_{NO,out}$.

$$G_{1,2} = \frac{k_{1,2}\left(s^2 + c_2 s + d_2\right)}{\left(s^2 + a_2 s + b_2\right)} \tag{89}$$

$$G_{2,2} = \frac{k_{2,2}\left(s + e_2\right)}{\left(s^2 + a_2 s + b_2\right)} \tag{90}$$

Table 8 Parameters of Equations (89) and (90)

Length*	$k_{1,2}$	a_2	b_2	c_2	d_2	e_2	$k_{2,2}$
$50\sqrt{2}$	0.022726	0.01104	3.935E-05	0.05717	1.45E-03	0.02987	-0.0010667
$100\sqrt{2}$	0.025472	0.0172	9.760E-05	0.09163	0.003475	0.04985	-0.0017724
$150\sqrt{2}$	0.027592	0.02387	1.884E-04	0.1286	0.006425	0.07173	-0.0025273
$200\sqrt{2}$	0.029329	0.03089	3.148E-04	0.1668	0.01031	0.09484	-0.0033225
$250\sqrt{2}$	0.030805	0.03812	4.785E-04	0.2054	0.01512	0.1187	-0.0041534
$300\sqrt{2}$	0.032094	0.04552	6.807E-04	0.2443	0.02083	0.1429	-0.0050166

* Length is the perpendicular length from stoichiometric line to nominal input

APPENDIX C

Nominal temperature is 498 K, and nominal space velocity is 30,000 /hr in all data of Appendix B.

APPENDIX C.1 - FIRST ORDER MODEL

Appendix C.1.1 – Model 1 (Region 1)

Transfer function relating $\delta C_{NH_3,in}$ to $\delta C_{NH_3,out}$ is as follows:

$$G_{1,1} = \frac{k_{1,1}\left(s + z_{1,1}\right)}{\left(s + p_{1,1}\right)}$$

Transfer function relating $\delta C_{NH_3,in}$ to $\delta C_{NO,out}$ is as follows:

$$G_{2,1} = \frac{k_{2,1}}{\left(s + p_{1,1}\right)}$$

Parameters for the above equations are as follows:

$$p_{1,1} = -1.151\times10^{-9} C_{NH3,in}^2 + 3.019\times10^{-6} C_{NH3,in} + 2.548\times10^{-4} \quad (91)$$

$$z_{1,1} = -5.558\times10^{-8} C_{NH3,in}^2 + 9.767\times10^{-5} C_{NH3,in} + 1.721\times10^{-2} \quad (92)$$

$$k_{1,1} = -8.493\times10^{-9} C_{NH3,in}^2 + 1.193\times10^{-5} C_{NH3,in} + 1.537\times10^{-2} \quad (93)$$

$$k_{2,1} = 1.039\times10^{-9} C_{NH3,in}^2 - 1.974\times10^{-6} C_{NH3,in} - 1.941\times10^{-4} \quad (94)$$

Appendix C.1.2 – Model 0 (Region 0)

Transfer function relating $\delta C_{NH_3,in}$ to $\delta C_{NH_3,out}$ is as follows:

$$G_{1.0} = \frac{k_{1.0}\left(s + z_{1.0}\right)}{\left(s + p_{1.0}\right)}$$

Transfer function relating $\delta C_{NH_3,in}$ to $\delta C_{NO,out}$ is as follows:

$$G_{2,0} = \frac{k_{2,0}}{\left(s + p_{1.0}\right)}$$

Parameters for the above equations are as follows:

$$p_{1.0} = 5.200\times10^{-9}l^2 + 2.448\times10^{-5}l - 3.240\times10^{-5} \quad (95)$$

$$z_{1.0} = -4.558\times10^{-10}l^3 + 4.306\times10^{-7}l^2 - 1.103\times10^{-4}l + 1.622\times10^{-2} \quad (96)$$

$$k_{1.0} = 4.543\times10^{-8}l^2 - 3.505\times10^{-5}l + 1.556\times10^{-2} \quad (97)$$

$$k_{2,0} = 6.667\times10^{-12}l^3 - 6.243\times10^{-9}l^2 + 1.913\times10^{-6}l - 1.972\times10^{-4} \quad (98)$$

where l is a perpendicular length from the stoichiometric line to the input condition.

Appendix C.1.3 – Model 2 (Region 2)

Transfer function relating $\delta C_{NH_3,in}$ to $\delta C_{NH_3,out}$ is as follows:

$$G_{1,2} = \frac{k_{1,2}\left(s + z_{1,2}\right)}{\left(s + p_{1,2}\right)}$$

Transfer function relating $\delta C_{NH_3,in}$ to $\delta C_{NO,out}$ is as follows:

$$G_{2,2} = \frac{k_{2,2}}{\left(s + p_{1,2}\right)}$$

Parameters for the above equations are as follows:

$$p_{1,2} = 6.621\times10^{-9} l^2 + 1.893\times10^{-5} l + 1.058\times10^{-3} \quad (99)$$

$$z_{1,2} = -1.204\times10^{-7} l^2 + 8.284\times10^{-4} l + 4.817\times10^{-2} \quad (100)$$

$$k_{1,2} = -3.522\times10^{-8} l^2 + 4.352\times10^{-5} l + 1.990\times10^{-2} \quad (101)$$

$$k_{2,2} = -1.192\times10^{-8} l^2 - 2.324\times10^{-5} l - 6.239\times10^{-4} \quad (102)$$

where l is a perpendicular length from the stoichiometric line to the input condition.

APPENDIX C.2 - SECOND ORDER MODEL

Appendix C.2.1 – Model 1 (Region 1)

Transfer function relating $\delta C_{NH_3,in}$ to $\delta C_{NH_3,out}$ is as follows:

$$G_{1,1} = \frac{k_{1,1}\left(s^2 + c_1 s + d_1\right)}{\left(s^2 + a_1 s + b_1\right)}$$

Transfer function relating $\delta C_{NH_3,in}$ to $\delta C_{NO,out}$ is as follows:

$$G_{2,1} = \frac{k_{2,1}\left(s + e_1\right)}{\left(s^2 + a_1 s + b_1\right)}$$

Parameters for the above equations are as follows:

$$k_{1,1} = -8.493\times10^{-9} C_{NH3,in}^2 + 1.193\times10^{-5} C_{NH3,in} + 1.537\times10^{-2} \quad (103)$$

$$k_{2,1} = 5.013\times10^{-10} C_{NH3,in}^2 - 1.035\times10^{-6} C_{NH3,in} - 1.064\times10^{-4} \quad (104)$$

$$a_1 = -5.294\times10^{-9} C_{NH3,in}^2 + 1.415\times10^{-5} C_{NH3,in} + 1.124\times10^{-3} \quad (105)$$

$$b_1 = 7.494\times10^{-12} C_{NH3,in}^2 + 2.215\times10^{-8} C_{NH3,in} - 5.989\times10^{-7} \quad (106)$$

$$c_1 = -3.249\times10^{-8} C_{NH3,in}^2 + 6.606\times10^{-5} C_{NH3,in} + 7.347\times10^{-3} \quad (107)$$

$$d_1 = -4.964\times10^{-11} C_{NH3,in}^2 + 8.329\times10^{-7} C_{NH3,in} - 8.554\times10^{-6} \quad (108)$$

$$e_1 = -1.387\times10^{-8} C_{NH3,in}^2 + 3.023\times10^{-5} C_{NH3,in} + 2.462\times10^{-3} \quad (109)$$

Appendix C.2.2 – Model 0 (Region 0)

Transfer function relating $\delta C_{NH_3,in}$ to $\delta C_{NH_3,out}$ is as follows:

$$G_{1,0} = \frac{k_{1,0}(s+c_0)(s+d_0)}{(s^2+a_0 s+b_0)}$$

Transfer function relating $\delta C_{NH_3,in}$ to $\delta C_{NO,out}$ is as follows:

$$G_{2,0} = \frac{k_{2,0}(s+e_0)}{(s^2+a_0 s+b_0)}$$

Parameters for the above equations are as follows:

$$k_{1,0} = 4.543\times10^{-8} l^2 - 3.505\times10^{-5} l + 1.556\times10^{-2} \quad (110)$$

$$k_{2,0} = 6.072\times10^{-12} l^3 - 5.744\times10^{-9} l^2 + 1.787\times10^{-6} l - 1.879\times10^{-4} \quad (111)$$

$$a_0 = -1.376\times10^{-8} l^2 + 2.749\times10^{-5} l + 3.826\times10^{-3} \quad (112)$$

$$b_0 = 1.100\times10^{-8} l^2 + 2.132\times10^{-5} l + 1.800\times10^{-6} \quad (113)$$

$$c_0 = 4.030\times10^{-8} l^2 - 1.136\times10^{-5} l + 1.061\times10^{-2} \quad (114)$$

$$d_0 = 3.753\times10^{-8} l^2 + 1.152\times10^{-6} l + 5.009\times10^{-3} \quad (115)$$

$$e_0 = 2.819\times10^{-8} l^2 + 7.733\times10^{-6} l + 4.963\times10^{-3} \quad (116)$$

where l is a perpendicular length from the stoichiometric line to the input condition.

Appendix C.2.3 – Model 2 (Region 2)

Transfer function relating $\delta C_{NH_3,in}$ to $\delta C_{NH_3,out}$ is as follows:

$$G_{1,2} = \frac{k_{1,2}\left(s^2 + c_2 s + d_2\right)}{\left(s^2 + a_2 s + b_2\right)}$$

Transfer function relating $\delta C_{NH_3,in}$ to $\delta C_{NO,out}$ is as follows:

$$G_{2,2} = \frac{k_{2,2}\left(s + e_2\right)}{\left(s^2 + a_2 s + b_2\right)}$$

Parameters for the above equations are as follows:

$$k_{1,2} = -3.522\times10^{-8} l^2 + 4.352\times10^{-5} l + 1.990\times10^{-2} \quad (117)$$

$$k_{2,2} = 2.574\times10^{-12} l^3 - 5.810\times10^{-9} l^2 - 8.850\times10^{-6} l - 4.126\times10^{-4} \quad (118)$$

$$a_2 = 3.014\times10^{-8} l^2 + 8.294\times10^{-5} l + 4.962\times10^{-3} \quad (119)$$

$$b_2 = 3.612\times10^{-9} l^2 + 2.069\times10^{-8} l + 2.086\times10^{-5} \quad (120)$$

$$c_2 = 1.026\times10^{-7} l^2 + 4.806\times10^{-4} l + 2.225\times10^{-2} \quad (121)$$

$$d_2 = 9.243\times10^{-8} l^2 + 9.083\times10^{-6} l + 3.450\times10^{-4} \quad (122)$$

$$e_2 = 1.036\times10^{-7} l^2 + 2.699\times10^{-4} l + 1.000\times10^{-2} \quad (123)$$

where l is a perpendicular length from the stoichiometric line to the input condition.

APPENDIX D

1. Nonlinear simulation

1.1. Flow Chart

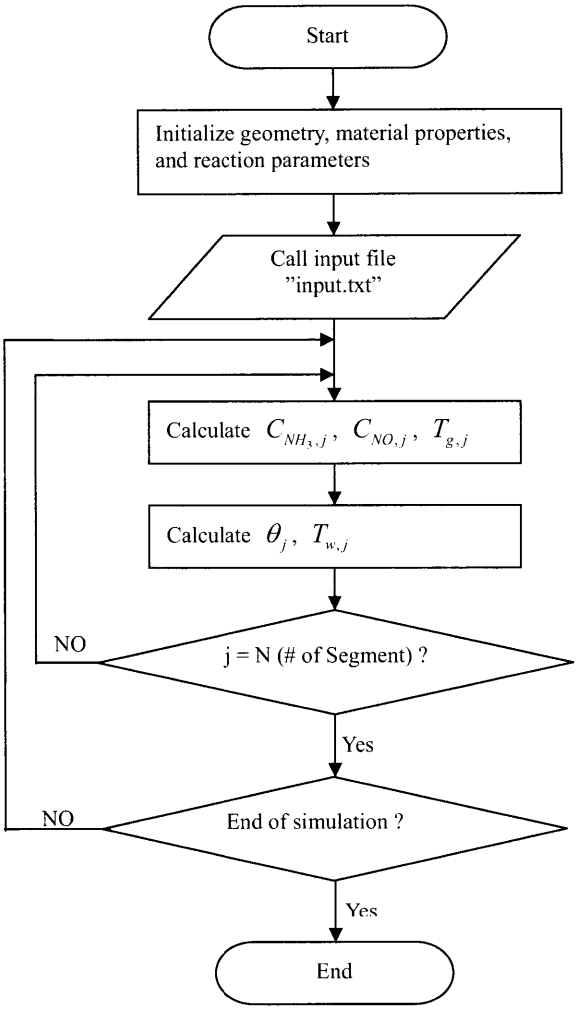

1.2. Code for MATLAB

```
% nonlinear simulation

% nonlinear model to simulate physical phenomoena in UREA SCR system.

% Author information
% Name : Hanbee Na (MIT ME Graduate Student)
% e-mail : hanbee.na@gmail.com
% Cell phone : 617-733-3571
% address : 70 Pacific St. #744B
%         cambridge, MA, 02139


% input data : "input.txt" which includes time, space velocity, input
% concentration of NH3 and NO, and gas temperature

% output data : "output.xls" which incldues time, NH3 and NO concentrration
% gas temperature at exit

% ********************
% ****** C ********
% ********************

% mass [kg]
% time [sec]
% length [m]
% concentration [mol] -> however, input & output [PPM]
% temperature [K]
% *energy [J]

% Date :   1) July 08, 2009
%         2) July 09, 2009
%            - Cnh3(i) modifiction : X1_2_1 & X1_2_2
%         3) July 21, 2009

% Four Reactions
% 1) Adsorption : NH3 => NH3(s)        : Ra
% 2) Desorption : NH3(s) => NH3        : Rd
% 3) Reduction  : 4NH3(s)+4NO+O2 => 4N2+6H2O    : Rr
% 4) Oxidation  : 2NH3(s)+1.5O2 -> N2 + 3H2O    : Ro


% Reaction rates in Arrhenius Type Equations
% 1) Adsorption : Ra = pa*(1-theta)*CNH3
% 2) Desorption : Rd = pd*exp(-Ed0(1-alpha*theta)/Ru/Tw)*theta
% 3) Reduction  : Rr = pr*exp(-Er/Ru/Tw)*theta*CNO
% 4) Oxidation  : Ro = po*exp(-Eo/Ru/Tw)*theta*CO2



clear all;
clc;

% reading properties data

NN = 20000; % maximum time to simulations

% time
Dt = 1.0D0;     % time inteval [sec]

% universal gas constant
```

```
R = 8.314D0;    % [J/mol/K]

% air properties at 250 oC ***temp***
rho_g = 0.675;  % density [kg/m^3]
Cp_g = 1034.0;  % heat capacity [J/kg/K]

% geometry
Ag = 9.4773E-7; % open channel area [m^2]
Dg = 1.098E-3;  % open channel diameter [m]
P = 3.449E-3;   % open channel perimeter [m]
N = 100;        % number of segments [ ]


length = 0.0254;% catalyst length [m]
Dx = length/N;  % delta_x [m]

Aw = 6.6517D-7;  % wall cross section area [m^2]


Aft_br = 1.0E0^2/4.0E0*pi();    % Catalyst front Area (inch^2)
Aft=Aft_br*(0.0254E0)^2;          % Catalyst front Area (m^2)
Volume = Aft*length;           % catalyst volume [m^3];

num_cell = 400*Aft_br;         % total number of cells (400 #psi)

% wall properties (Codierite raw material?)
rho_w = 1800.0; % density [kg/m^3]
Cp_w = 1050.0;    % heat capacity [J/kg/K]
k_w = 0.419;    % conductivity [W/m/K]


% others
u = 0.3603;     % gas velocity [m/s]
h = 167;       % heat transfer coefficient [W/m^2/K]

%%temp
h=10;

% density of sites
den = 0.001;    % density of sites [mole-sites/m^2]



% correction factor for pre-exponetial factors
temp = 1.0E0;

% reaction constants from hanbee's values
% adsorption
Ea = 0.0;       % activation energy
p_a = 0.25;   % *** temp *** ==>

% desorption [Low Temperature]
Ed0 = 101000.0; % activation energy [J/mol]
p_d = 1400000; % pre-exponential factor ==> good

alpha = 0.7;

% Reduction
Er = 79000.0;
p_r = 150000000.0;

% Oxidation
Eo = 140000.0;
```

```
p_o = 2.2E8;



% maximum capacity to adsorb NH3,

% ***********************************
OMEGA = 1.4E-5;   % [mole-sites/cell]


% ***********************************

%Theta = OMEGA/N;       % [mole-sites/cell/segment]
Theta = OMEGA/length;   % [mole-sites/m]
s=Theta;               % same to Theta [mole-sites/m]



% input data
% [input2,input3,input4,input5] = textread('input.txt','%f%f%f%f');
[input1,input2,input3,input4,input5] = textread('input.txt','%d%f%f%f%f');

% time_in=input(:,1);         % first column : time [sec]
% u_in=input(:,2)*1.201E-5;  % SV : 30,000 [/Hr] = 0.3603 [m/s] (in a cell)
% Cnh3_in=input(:,3);   % NH3 input concentration : [PPM] into [mol]
% Cno_in=input(:,4);    % NO input concentration :  [PPM] into [mol]
% Tg_in=input(:,5);           % input gas temperature [K]
% [M,M2]=size(u_in);          % number of data

% u_in=input2*1.201E-5;   % SV : at 30,000 [/Hr] = 0.3603 [m/s] (in a cell)
% Cnh3_in=input3;         % NH3 input concentration : [PPM] into [mol]
% Cno_in=input4;          % NO input concentration :  [PPM] into [mol]
% Tg_in=input5;           % input gas temperature [K]

Time_in = input1;       % Time input
SV_in   = input2;       % space velocity
PPM_nh3_in = input3;    % NH3 input mole fraction in PPM [PPM]
PPM_no_in = input4;     % NO input mole fraction in PPM [PPM]
Tg_in=input5;           % input gas temperature [K]

Xnh3_in = PPM_nh3_in/1.0E6; % NH3 input mole fraction
Xno_in = PPM_no_in/1.0E6;  % NO input mole fraction

[MM, MM2] = size(input3);

MOLEMASS_AIR = 28.97E0; % Molecular MASS of AIR [kg/kmol]
rho_g_STP = 1.293E0;    % Gas density at STP

for m=1:NN %MM
rho_g(m)=354.6E0/Tg_in(m);   % density(Tg_in) [kg/m^3]
Mass_input(m)=SV_in(m)/3600.0E0*Volume*rho_g_STP;   % Total Mass input [Kg/s]
mass_input_cell(m)=Mass_input(m)/num_cell;   % Mass flow rate per cell [Kg/s]

q_input_cell(m)=mass_input_cell(m)/rho_g(m); %flow rate per cell [m^3/s]
u_in(m) = q_input_cell(m)/Ag;           % flow velocity [m/s]

Cair_in(m) = rho_g(m)/MOLEMASS_AIR*1.0E3;
Cnh3_in(m) = Cair_in(m)*Xnh3_in(m);
Cno_in(m) = Cair_in(m)*Xno_in(m);
Co2_in(m) = Cair_in(m)*0.08;
end
```

```
% variables initialization
% X1 group
Tg_o    = zeros(1,N);   % old gas Temeprature [K]
Tg      = zeros(1,N);   % gas Temperature [K]
Cnh3_o  = zeros(1,N);   % old NH3 concentration [mol/m^3]
Cnh3    = zeros(1,N);   % NH3 concentration [mol/m^3]
Cno_o   = zeros(1,N);   % old NO concentration [mol/m^3]
Cno     = zeros(1,N);   % NO concentration [mol/m^3]

% X2 group
Tw_o    = zeros(1,N);   % old wall temperature [K]
Tw      = zeros(1,N);   % wall temperature [K]
theta_o = zeros(1,N);   % old surface faction [ ]
theta   = zeros(1,N);   % surface fraction [ ]

% intermediate variables
X1_1_1  = zeros(1,N);   % to obtain Tg distribution #1
X1_1_2  = zeros(1,N);   % to obtain Tg distriubtion #2

X1_2_1  = zeros(1,N);   % to obtain NH3 distribution #1
X1_2_2  = zeros(1,N);   % to obtain NH3 distribution #2

X1_3_1  = zeros(1,N);   % to obtain NO distribution


X2_1_1  = zeros(1,N);   % to obtain new Tw information #1
X2_1_2  = zeros(1,N);   % to obtain new Tw information #2

X2_2_1  = zeros(1,N);   % to obtain new theta information

% initialize wall temperature and theta
for j=1:N

    Tw(j) = 473.0D0;    % Tw = 200 oC
    % theta = 0
    theta(j) = 0.0D0;

end

    Tw_o = Tw;         % old time data
    theta_o = theta;    % old time data

k1=0;
k2=0;

for i=1:NN %M


    % calculate gas properties (input temperature)
    Cp_g = 1034E0; % heat capacity [kJ/ksg/K] @ at 250 oC
    k_g=6.70E-5*Tg_in(i)+6.79E-3; % conductivity(Tg_in) [W/m/K]




    k1=k1+1;

    if (k1>1000)
        k1=0;
        k2=k2+1;
        k2*1000
    end
```

```
    % update heat transfer coefficient
    % Nu number = 48/11
    h=48/11/Dg*k_g;

    %%temp
    %h=10;

    u =  u_in(i);   % flow velocity [m/s]

    MOLE = rho_g/28.97*1.0E3; %28.97 air molecular weight [mole/m^3]


    for j=1:N


        if (j==1)

            % X2_2_1(1) = 1+den*P*Dt/Theta*(p_a*Cnh3_in(i)+p_d*exp(-Ed0*(1.0D0-
alpha*theta(1)/R/Tw(j))+p_r*exp(-Er/R/Tw(j))*Cno_in(i)+p_o*exp(-
Eo/R/Tw(j))*Co2));
            % correction
            X2_2_1(1) = 1+Dt*(p_a*Cnh3_in(i)+p_d*exp(-Ed0*(1.0D0-
alpha*theta(1))/R/Tw(1))+p_r*exp(-Er/R/Tw(1))*Cno_in(i)+p_o*exp(-
Eo/R/Tw(1))*Co2_in(i));

            % X2_2_2(1) = den*P*Dt/Theta*p_a*Cnh3_in(i);
            % correction
            X2_2_2(1) = Dt*p_a*Cnh3_in(i);

        end


        X1_1_1(j) = rho_g(i)*Ag*Cp_g*u/(rho_g(i)*Ag*Cp_g*u+h*P*Dx);
        X1_1_2(j) = h*P*Dx/(rho_g(i)*Ag*Cp_g*u+h*P*Dx);

        X1_2_1(j) = Ag*u/(Ag*u+s*Dx*p_a*(1.0D0-theta(j)));
        X1_2_2(j) = s*Dx*p_d*exp(-Ed0*(1-
alpha*theta(j))/R/Tw(j))*theta(j)/(Ag*u+s*Dx*p_a*(1.0D0-theta(j)));

        X1_3_1(j) = Ag*u/(Ag*u+s*p_r*Dx*exp(-Er/R/Tw(j))*theta(j));


        X2_1_1(j) = rho_w*Aw*Cp_w/(rho_w*Aw*Cp_w+h*P*Dt);
        X2_1_2(j) = h*P*Dt/(rho_w*Aw*Cp_w+h*P*Dt);

    end


    for j=2:N

        X2_2_1(j) = 1+Dt*(p_a*Cnh3(j-1)+p_d*exp(-Ed0*(1.0D0-
alpha*theta(j))/R/Tw(j))+p_r*exp(-Er/R/Tw(j))*Cno(j-1)+p_o*exp(-
Eo/R/Tw(j))*Co2_in(i));
        X2_2_2(j) = Dt*p_a*Cnh3(j-1);

    end


    % temp

        X2_2_1_data(i)=X2_2_1(1);

    % X1 distribution
```

```
    % at the first segment

        % gas temperature at j=1 [K]
        Tg(1) = X1_1_1(1)*Tg_in(i)+X1_1_2(1)*Tw(1);

        % NH3 concentration at j=1 [mol/m^3]
        Cnh3(1) = X1_2_1(1)*Cnh3_in(i)+X1_2_2(1);

        % NO concentration at j=1 [mol/m^3]
        Cno(1) = X1_3_1(1)*Cno_in(i);

%       % from i=2 to end of segments
          Cnh3_1_data(i)=Cnh3(1)/MOLE(i)*1.0E6;

    for j=1:N-1

        % Gas temperature at j [K]
        Tg(j+1) = X1_1_1(j+1)*Tg(j)+X1_1_2(j+1)*Tw(j+1);

        % NH3 concentration at j=1 [mol/m^3]
        Cnh3(j+1) = X1_2_1(j+1)*Cnh3(j)+X1_2_2(j+1);

        % NO concentration at j=1 [mol/m^3]
        Cno(j+1) = X1_3_1(j+1)*Cno(j);



    end

    % X2 update
    % at the first segment

        % wall temperature at j=1 [K]
        Tw(1) = X2_1_1(1)*Tw_o(1)+X2_1_2(1)*Tg_in(i);

        % theta at j=1 [ ]
        %theta(1) =  1/X2_2_1(1)*Dt/Theta*p_a*Cnh3(1)+1/X2_2_1(1)*theta_o(1);
        theta(1) = theta_o(1)/X2_2_1(1)+ X2_2_2(1)/X2_2_1(1);

    for j=2:N

        % wall temperature at j [K]
        Tw(j) = X2_1_1(j)*Tw_o(j)+X2_1_2(j)*Tg(j-1);

        % theta at j
        %theta(j) =  1/X2_2_1(j)*Dt/Theta*p_a*Cnh3(j)+1/X2_2_1(j)*theta_o(j);
        %theta(j) = X2_2_2(j)/X2_2_1(j);
        theta(j) = theta_o(j)/X2_2_1(j)+ X2_2_2(j)/X2_2_1(j);



    end


    % data recording
    % all data
%     for j=1:N
%        Tg_data(i,j)=Tg(j);     % Tg data recording [K]
%        Cnh3_data(i,j)=Cnh3(j); % NH3 data recording [mol/m^3]
%        Cno_data(i,j)=Cno(j);   % NO data recording [mol/m^3]
%
%        Tw_data(i,j)=Tw(j);     % Tw  data recording [K}
%        theta_data(i,j)=theta(j); % theta data recording [ ]
%
```

```
% %    end
%       if (i>46000 && i<50000)
%
%         Tg_data(i,:)=Tg(1,:)';      % Tg data recording [K]
%         Cnh3_data(i,:)=Cnh3(1,:)'/(rho_g/28.97*1000/1.0d6);  % NH3 data
recording [mol/m^3]
%         Cno_data(i,:)=Cno(1,:)'/(rho_g/28.97*1000/1.0d6);    % NO data
recording [mol/m^3]
% %
%         Tw_data(i,:)=Tw(1,:)';      % Tw  data recording [K}
%         theta_data(i,:)=theta(1,:)';% theta data recording [ ]
%       end
%    i;
%    % exit information
       Tg_out(i,1)=Tg(1,N);       % Tg at exit [K]
%       Cnh3_out(i,1)=Cnh3(1,N);    % NH3 concentration at exit [mol/m^3]
%       Cno_out(i,1)=Cno(1,N);     % NO concentration at exit [mol/m^3]



%
%
      Cnh3_out_ppm(i,1)=Cnh3(1,N)/(rho_g(i)/28.97*1000/1.0d6);  % NH3
concentration at exit [PPM]
      Cno_out_ppm(i,1)=Cno(1,N)/(rho_g(i)/28.97*1000/1.0d6);    % NO
concentration at exit [PPM]

      Cnh3_out(i,1)=Cnh3(1,N);
      Cno_out(i,1)=Cno(1,N);


   % X2's old data update
      Tw_o=Tw;              % Tw data update [K]
      theta_o=theta;         % theta update [ ]
% Cnh3_in_ppm(i,1)=Cnh3_in(i)*1.0E6/MOLE;
% Cno_in_ppm(i,1)=Cno_in(i)*1.0E6/MOLE;

end

output(1:NN,1) = input1(1:NN,1);
output(1:NN,2) = Cnh3_out_ppm';        % NH3 concentration at exit [PPM]
output(1:NN,3) = Cno_out_ppm';         % NO concentration at exit [PPM]
output(1:NN,4) = Tg_out;             % Tg at exit [K]

% dlmwrite('output.txt', output(:,1))
dlmwrite('output.txt', output, 'delimiter', '\t')


%End of Simulation
```

2. Code for Linearized system & Reduced order system

2.1. Flow Chart

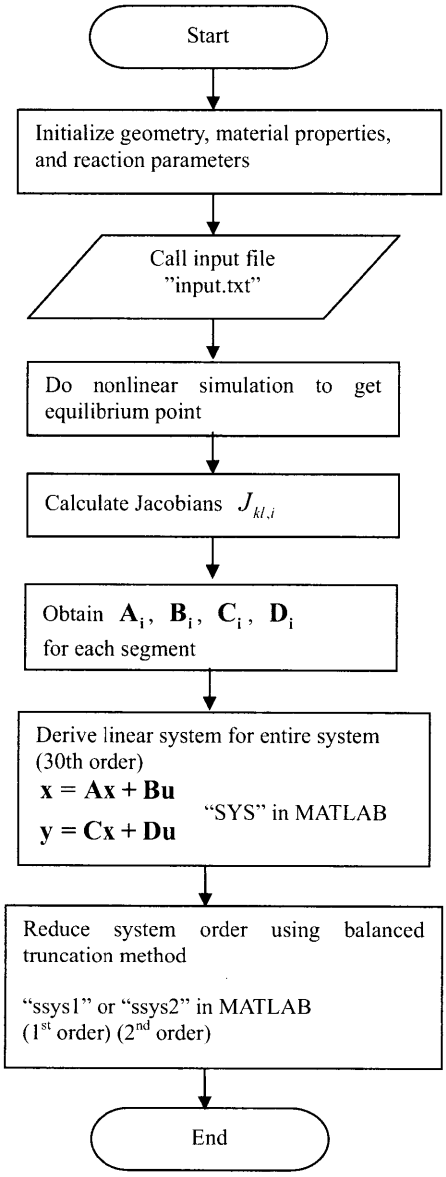

2.2. Code for MATLAB

```
% high order linearized model and reduced order model

% Author information
% Name : Hanbee Na (MIT ME Graduate Student)
% e-mail : hanbee.na@gmail.com
% Cell phone : 617-733-3571
% address : 70 Pacific St. #744B
%          cambridge, MA, 02139


% input data : "input.xls" which includes time, space velocity, input
% concentration of NH3 and NO, and gas temperature

% output data : "output.xls" which incldues time, NH3 and NO concentrration
% gas temperature at exit

% mass [kg]
% time [sec]
% length [m]
% concentration [mol] -> however, input & output [PPM]
% temperature [K]
% *energy [J]

clear all;
clc;


% reading properties data

% time
Dt = 1.0D0;     % time inteval [sec]

% universal gas constant
R = 8.314D0;    % [J/mol/K]

% air properties at 250 oC ***temp***
rho_g = 0.675;  % density [kg/m^3]
Cp_g = 1034.0;  % heat capacity [J/kg/K]

% geometry
Ag = 9.4773E-7; % open channel area [m^2]
Dg = 1.098E-3;  % open channel diameter [m]
P = 3.449E-3;   % open channel perimeter [m]

N=15;          % 15 Segments



length = 0.0254;% catalyst length [m]
Dx = length/N;  % delta_x [m]

Aw = 6.6517D-7;  % wall cross section area [m^2]


Aft_br = 1.0E0^2/4.0E0*pi();    % Catalyst front Area (inch^2)
Aft=Aft_br*(0.0254E0)^2;          % Catalyst front Area (m^2)
Volume = Aft*length;           % catalyst volume [m^3];

num_cell = 400*Aft_br;         % total number of cells (400 #psi)

% wall properties (Codierite raw material?)
```

```
rho_w = 1800.0; % density [kg/m^3]
Cp_w = 1050.0;    % heat capacity [J/kg/K]
k_w = 0.419;    % conductivity [W/m/K]



% others
u = 0.3603;     % gas velocity [m/s]
h = 167;       % heat transfer coefficient [W/m^2/K]

%%temp
h=10;

% density of sites
den = 0.001;    % density of sites [mole-sites/m^2]



alpha = 0.7;


% reaction constants from hanbee's values
% adsorption
Ea = 0.0;       % activation energy
p_a = 0.25;   % *** temp *** ==>

% desorption [Low Temperature]
Ed0 = 101000.0; % activation energy [J/mol]
p_d = 1400000; % pre-exponential factor ==> good

alpha = 0.7;

% Reduction
Er = 79000.0;
p_r = 150000000.0;

% Oxidation
Eo = 140000.0;
p_o = 2.2E8;


% maximum capacity to adsorb NH3,

% ***********************************


OMEGA = 1.4E-5;          % [mole-sites/cell]




%OMEGA = OMEGA*1/13;


% ***********************************

%Theta = OMEGA/N;       % [mole-sites/cell/segment]
Theta = OMEGA/length;   % [mole-sites/m]
s=Theta;              % same to Theta [mole-sites/m]
```

```
% input data
% [input2,input3,input4,input5] = textread('input.txt','%f%f%f%f');
[input1,input2,input3,input4,input5] = textread('input.txt','%d%f%f%f%f');


Time_in = input1;      % Time input
SV_in   = input2;      % space velocity
PPM_nh3_in = input3;    % NH3 input mole fraction in PPM [PPM]
PPM_no_in = input4;     % NO input mole fraction in PPM [PPM]
Tg_in=input5;          % input gas temperature [K]

Xnh3_in = PPM_nh3_in/1.0E6; % NH3 input mole fraction
Xno_in = PPM_no_in/1.0E6;  % NO input mole fraction

[MM, MM2] = size(input3);

MOLEMASS_AIR = 28.97E0; % Molecular MASS of AIR [kg/kmol]
rho_g_STP = 1.293E0;    % Gas density at STP3

for m=1:10000 %MM
rho_g(m)=354.6E0/Tg_in(m);   % density(Tg_in) [kg/m^3]
Mass_input(m)=SV_in(m)/3600.0E0*Volume*rho_g_STP;   % Total Mass input [Kg/s]
mass_input_cell(m)=Mass_input(m)/num_cell;   % Mass flow rate per cell [Kg/s]

q_input_cell(m)=mass_input_cell(m)/rho_g(m); %flow rate per cell [m^3/s]
u_in(m) = q_input_cell(m)/Ag;           % flow velocity [m/s]

Cair_in(m) = rho_g(m)/MOLEMASS_AIR*1.0E3;
Cnh3_in(m) = Cair_in(m)*Xnh3_in(m);
Cno_in(m) = Cair_in(m)*Xno_in(m);
Co2_in(m) = Cair_in(m)*0.08;
end


% variables initialization
% X1 group
Tg_o    = zeros(1,N);   % old gas Temeprature [K]
Tg      = zeros(1,N);   % gas Temperature [K]
Cnh3_o  = zeros(1,N);   % old NH3 concentration [mol/m^3]
Cnh3    = zeros(1,N);   % NH3 concentration [mol/m^3]
Cno_o   = zeros(1,N);   % old NO concentration [mol/m^3]
Cno     = zeros(1,N);   % NO concentration [mol/m^3]

% X2 group
Tw_o    = zeros(1,N);   % old wall temperature [K]
Tw      = zeros(1,N);   % wall temperature [K]
theta_o = zeros(1,N);    % old surface faction [ ]
theta   = zeros(1,N);   % surface fraction [ ]

% intermediate variables
X1_1_1  = zeros(1,N);   % to obtain Tg distribution #1
X1_1_2  = zeros(1,N);   % to obtain Tg distriubtion #2

X1_2_1  = zeros(1,N);   % to obtain NH3 distribution #1
X1_2_2  = zeros(1,N);   % to obtain NH3 distribution #2

X1_3_1  = zeros(1,N);   % to obtain NO distribution


X2_1_1  = zeros(1,N);   % to obtain new Tw information #1
X2_1_2  = zeros(1,N);   % to obtain new Tw information #2

X2_2_1  = zeros(1,N);   % to obtain new theta information
```

```
% initialize wall temperature and theta
for j=1:N

    Tw(j) = 498.0D0;    % Tw = 200 oC
    % theta = 0
    theta(j) = 0.0D0;

end

    Tw_o = Tw;          % old time data
    theta_o = theta;    % old time data

k1=0;
k2=0;

for i=1:10000 %M


    % calculate gas properties (input temperature)
    Cp_g = 1034E0; % heat capacity [kJ/ksg/K] @ at 250 oC
    k_g=6.70E-5*Tg_in(i)+6.79E-3; % conductivity(Tg_in) [W/m/K]




    k1=k1+1;

    if (k1>1000)
        k1=0;
        k2=k2+1;
        k2*1000
    end

    % update heat transfer coefficient
    % Nu number = 48/11
    h=48/11/Dg*k_g;

    %%temp
    %h=10;

    u =  u_in(i);   % flow velocity [m/s]

    MOLE = rho_g/28.97*1.0E3; %28.97 air molecular weight [mole/m^3]


    for j=1:N


        if (j==1)

            % X2_2_1(1) = 1+den*P*Dt/Theta*(p_a*Cnh3_in(i)+p_d*exp(-Ed0*(1.0D0-
alpha*theta(1)/R/Tw(j))+p_r*exp(-Er/R/Tw(j))*Cno_in(i)+p_o*exp(-
Eo/R/Tw(j))*Co2));
            % correction
            X2_2_1(1) = 1+Dt*(p_a*Cnh3_in(i)+p_d*exp(-Ed0*(1.0D0-
alpha*theta(1))/R/Tw(1))+p_r*exp(-Er/R/Tw(1))*Cno_in(i)+p_o*exp(-
Eo/R/Tw(1))*Co2_in(i));

            % X2_2_2(1) = den*P*Dt/Theta*p_a*Cnh3_in(i);
            % correction
            X2_2_2(1) = Dt*p_a*Cnh3_in(i);
```

```
        end


        X1_1_1(j) = rho_g(i)*Ag*Cp_g*u/(rho_g(i)*Ag*Cp_g*u+h*P*Dx);
        X1_1_2(j) = h*P*Dx/(rho_g(i)*Ag*Cp_g*u+h*P*Dx);

        X1_2_1(j) = Ag*u/(Ag*u+s*Dx*p_a*(1.0D0-theta(j)));
        X1_2_2(j) = s*Dx*p_d*exp(-Ed0*(1-
alpha*theta(j))/R/Tw(j))*theta(j)/(Ag*u+s*Dx*p_a*(1.0D0-theta(j)));

        X1_3_1(j) = Ag*u/(Ag*u+s*p_r*Dx*exp(-Er/R/Tw(j))*theta(j));


        X2_1_1(j) = rho_w*Aw*Cp_w/(rho_w*Aw*Cp_w+h*P*Dt);
        X2_1_2(j) = h*P*Dt/(rho_w*Aw*Cp_w+h*P*Dt);

    end


    for j=2:N

        X2_2_1(j) = 1+Dt*(p_a*Cnh3(j-1)+p_d*exp(-Ed0*(1.0D0-
alpha*theta(j))/R/Tw(j))+p_r*exp(-Er/R/Tw(j))*Cno(j-1)+p_o*exp(-
Eo/R/Tw(j))*Co2_in(i));
        X2_2_2(j) = Dt*p_a*Cnh3(j-1);

    end


    % temp

        X2_2_1_data(i)=X2_2_1(1);

    % X1 distribution
    % at the first segment

        % gas temperature at j=1 [K]
        Tg(1) = X1_1_1(1)*Tg_in(i)+X1_1_2(1)*Tw(1);

        % NH3 concentration at j=1 [mol/m^3]
        Cnh3(1) = X1_2_1(1)*Cnh3_in(i)+X1_2_2(1);

        % NO concentration at j=1 [mol/m^3]
        Cno(1) = X1_3_1(1)*Cno_in(i);

%       % from i=2 to end of segments
          Cnh3_1_data(i)=Cnh3(1)/MOLE(i)*1.0E6;

    for j=1:N-1

        % Gas temperature at j [K]
        Tg(j+1) = X1_1_1(j+1)*Tg(j)+X1_1_2(j+1)*Tw(j+1);

        % NH3 concentration at j=1 [mol/m^3]
        Cnh3(j+1) = X1_2_1(j+1)*Cnh3(j)+X1_2_2(j+1);

        % NO concentration at j=1 [mol/m^3]
        Cno(j+1) = X1_3_1(j+1)*Cno(j);



    end
```

```
    % X2 update
    % at the first segment

        % wall temperature at j=1 [K]
        Tw(1) = X2_1_1(1)*Tw_o(1)+X2_1_2(1)*Tg_in(i);

        % theta at j=1 [ ]
        %theta(1) =  1/X2_2_1(1)*Dt/Theta*p_a*Cnh3(1)+1/X2_2_1(1)*theta_o(1);
        theta(1) = theta_o(1)/X2_2_1(1)+ X2_2_2(1)/X2_2_1(1);

    for j=2:N

        % wall temperature at j [K]
        Tw(j) = X2_1_1(j)*Tw_o(j)+X2_1_2(j)*Tg(j-1);

        % theta at j
        %theta(j) =  1/X2_2_1(j)*Dt/Theta*p_a*Cnh3(j)+1/X2_2_1(j)*theta_o(j);
        %theta(j) = X2_2_2(j)/X2_2_1(j);
        theta(j) = theta_o(j)/X2_2_1(j)+ X2_2_2(j)/X2_2_1(j);



    end


%     % exit information
         Tg_out(i,1)=Tg(1,N);       % Tg at exit [K]
%        Cnh3_out(i,1)=Cnh3(1,N);    % NH3 concentration at exit [mol/m^3]
%        Cno_out(i,1)=Cno(1,N);      % NO concentration at exit [mol/m^3]
%
%
       Cnh3_out_ppm(i,1)=Cnh3(1,N)/(rho_g(i)/28.97*1000/1.0d6);  % NH3
concentration at exit [PPM]
       Cno_out_ppm(i,1)=Cno(1,N)/(rho_g(i)/28.97*1000/1.0d6);    % NO
concentration at exit [PPM]

       Cnh3_out(i,1)=Cnh3(1,N);
       Cno_out(i,1)=Cno(1,N);


    % X2's old data update
       Tw_o=Tw;              % Tw data update [K]
       theta_o=theta;         % theta update [ ]
% Cnh3_in_ppm(i,1)=Cnh3_in(i)*1.0E6/MOLE;
% Cno_in_ppm(i,1)=Cno_in(i)*1.0E6/MOLE;

end

Cnh3=Cnh3';
Cno=Cno';
theta=theta';

Cnh3_eq(1,1)=Cnh3_in(i);
Cno_eq(1,1)=Cno_in(i);


% initialize System Matrixes
A11=zeros(3,3,N);
A12=zeros(3,2,N);
A21=zeros(2,3,N);
A22=zeros(2,2,N);
```

```
%
AA1=zeros(3,3,N);
AA2=zeros(3,2,N);
AA3=zeros(2,2,N);
AA4=zeros(2,3,N);


X1=zeros(3,1,N+1);
x1=zeros(3,1,N);
x1_p=zeros(3,1,N+1);  % p stands for previous
X1_eq=zeros(3,1,N); % Equilibrium operating point;

X1_d=zeros(3,1,N+1);  % X1 distribution (including input condition)


X2=zeros(2,1,N);
x2=zeros(2,1,N);
x2_p=zeros(2,1,N);  % p stands for previous
X2_eq=zeros(2,1,N); % Equilibrium operating point;

J11=zeros(N,1);
J12=zeros(N,1);

J21=zeros(N,1);
J22=zeros(N,1);
J23=zeros(N,1);
J24=zeros(N,1);

tt=zeros(N,1);

J31=zeros(N,1);
J32=zeros(N,1);

J41=zeros(N,1);
J42=zeros(N,1);
J43=zeros(N,1);
J44=zeros(N,1);

J51=zeros(N,1);
J52=zeros(N,1);
J53=zeros(N,1);
J54=zeros(N,1);

%% input of nominal condition

X1_eq(2,1,1)=Cnh3_in(i);
X1_eq(3,1,1)=Cno_in(i);

Co2_eq= 1.9633;
u_in_eq=u_in(i);
rho_g=rho_g(i);

for k=1:N
    X1_eq(1,1,k)=498.0;
    X2_eq(1,1,k)=498.0;

    X2_eq(2,1,k)=theta(k);

    X1_eq(2,1,k+1)=Cnh3(k);
    X1_eq(3,1,k+1)=Cno(k);
end;
```

```
% Subroutine to calculate Jacobian
for j=1:N


    tt(j)=1.0D0+Dt*p_a*X1_eq(2,1,j)+Dt*p_d*exp(-Ed0*(1.0D0-
alpha*X2_eq(2,1,j))/R/X2_eq(1,1,j))+Dt*p_r*exp(-
Er/R/X2_eq(1,1,j))*X1_eq(3,1,j)+Dt*p_o*exp(-Eo/R/X2_eq(1,1,j))*Co2_eq;
    %J21(j)=1.0D0/tt(j)-(X2_eq(2,1,j)+Dt*p_a*X1_eq(2,1,j))*exp(-Ed0*(1.0D0-
alpha*X2_eq(2,1,j))/R/X2_eq(1,1,j))*Dt*p_d*(Ed0*alpha/8.314/X2_eq(1,1,j))/tt(j
)^2;
    J11(j)=1.0D0/tt(j)-(X2_eq(2,1,j)+Dt*p_a*X1_eq(2,1,j))*exp(-Ed0*(1.0D0-
alpha*X2_eq(2,1,j))/R/X2_eq(1,1,j))*Dt*p_d*(Ed0*alpha/R/X2_eq(1,1,j))/tt(j)^2;
    J111=1.0/tt(j);
    J112=(X2_eq(2,1,j)+Dt*p_a*X1_eq(2,1,j))*exp(-Ed0*(1.0D0-
alpha*X2_eq(2,1,j))/R/X2_eq(1,1,j))*Dt*p_d*(Ed0*alpha/R/X2_eq(1,1,j))/tt(j)^2;

    J11(j)=J111-J112;

    J11temp1=-p_a*X1_eq(2,1,j);
    J11temp2=-p_d*exp(-Ed0*(1.0D0-alpha*X2_eq(2,1,j))/R/X2_eq(1,1,j));
    J11temp3=-p_d*exp(-Ed0*(1.0D0-
alpha*X2_eq(2,1,j))/R/X2_eq(1,1,j))*X2_eq(2,1,j)*alpha*Ed0/R/X1_eq(1,1,j);
    J11temp4=-p_r*exp(-Er/R/X2_eq(1,1,j))*X1_eq(3,1,j);
    J11temp5=-p_o*exp(-Eo/R/X2_eq(1,1,j))*Co2_eq;

    J11t(j)=J11temp1+J11temp2+J11temp3+J11temp4+J11temp5;


    J12(j)=-(X2_eq(2,1,j)+Dt*p_a*X1_eq(2,1,j))/tt(j)^2*(Dt*p_d*exp(-
Ed0*(1.0D0-alpha*X2_eq(2,1,j))/R/X2_eq(1,1,j))*Ed0*(1-
alpha*X2_eq(2,1,j))/R/X2_eq(1,1,j)^2+Dt*p_r*exp(-
Er/R/X2_eq(1,1,j))*X1_eq(3,1,j)*Er/R/X1_eq(1,1,j)^2+Dt*p_o*exp(-
Eo/R/X2_eq(1,1,j))*Co2_eq*Eo/R/X2_eq(1,1,j)^2);

    J12temp1=-p_d*exp(-Ed0*(1.0d0-
alpha*X2_eq(2,1,j))/R/X2_eq(1,1,j))*X2_eq(2,1,j)*(1.0d0-
alpha*X2_eq(2,1,j))/R/X2_eq(1,1,j)^2.0;
    J12temp2=-p_r*exp(-Er/R/X2_eq(1,1,j))*X1_eq(3,1,j)*Er/R/X2_eq(1,1,j)^2;
    J12temp3=-p_o*exp(-Eo/R/X2_eq(1,1,j))*Co2_eq*Eo/R/X2_eq(1,1,j)^2;

    J12t(j)=J12temp1+J12temp2+J12temp3;


    J13(j)=Dt*p_a/tt(j)-(X2_eq(2,1,j)+Dt*p_a*X1_eq(2,1,j))*Dt*p_a/tt(j)^2;

    J13t(j)=p_a*(1.0d0-X2_eq(2,1,j));


    J14(j)=-(X2_eq(2,1,j)+Dt*p_a*X1_eq(2,1,j))*Dt*p_r*exp(-
Er/R/X2_eq(1,1,j))/tt(j)^2;

    J14t(j)=-p_r*exp(-Er/R/X2_eq(1,1,j))*X2_eq(2,1,j);



    J22(j)=rho_w*Aw*Cp_w/(rho_w*Aw*Cp_w+h*P*Dt);

    J22t(j)=-h*P/(rho_w*Aw*Cp_w);


    J25(j)=h*P*Dt/(rho_w*Aw*Cp_w+h*P*Dt);
```

```
    J25t(j)=h*P/(rho_w*Aw*Cp_w);

    ttt=Ag*u_in_eq+s*Dx*p_a*(1-X2_eq(2,1,j));
    J31(j)=Ag*u_in_eq*s*Dx*p_a*X1_eq(2,1,j)/ttt^2+(s*Dx*p_d)^2/ttt^2*exp(-
Ed0*(1.0D0-
alpha*X2_eq(2,1,j))/R/X2_eq(1,1,j))*X2_eq(2,1,j)+s*Dx*p_d/ttt*Ed0*alpha/R/X2_e
q(1,1,j)*exp(-Ed0*(1.0D0-
alpha*X2_eq(2,1,j))/R/X2_eq(1,1,j))*X2_eq(2,1,j)+s*Dx*p_d/ttt*exp(-Ed0*(1.0D0-
alpha*X2_eq(2,1,j))/R/X2_eq(1,1,j));

    J311=Ag*u_in_eq*s*Dx*p_a*X1_eq(2,1,j)/ttt^2;
    J312=(s*Dx)^2*p_d*p_a/ttt^2*exp(-Ed0*(1-
alpha*X2_eq(2,1,j))/R/X2_eq(1,1,j))*X2_eq(2,1,j);
    J313=(s*Dx*p_d)/ttt*Ed0*alpha/R/X2_eq(1,1,j)*exp(-Ed0*(1-
alpha*X2_eq(2,1,j))/R/X2_eq(1,1,j))*X2_eq(2,1,j);
    J314=(s*Dx*p_d)/ttt*exp(-Ed0*(1-alpha*X2_eq(2,1,j))/R/X2_eq(1,1,j));

    J31(j)=J311+J312+J313+J314;

    J31temp1=(s/Ag/u_in_eq)*p_a*X1_eq(2,1,j);
    J31temp2=(s/Ag/u_in_eq)*p_d*exp(-Ed0*(1-
alpha*X2_eq(2,1,j))/R/X2_eq(1,1,j));
    J31temp3=(s/Ag/u_in_eq)*p_d*exp(-Ed0*(1-
alpha*X2_eq(2,1,j))/R/X2_eq(1,1,j))*X2_eq(2,1,j)*Ed0*alpha/R/X2_eq(1,1,j);
    J31t(j)=J31temp1+J31temp2+J31temp3;


    J32(j)=s*Dx*p_d/ttt*exp(-Ed0*(1.0D0-
alpha*X2_eq(2,1,j))/R/X2_eq(1,1,j))*X2_eq(2,1,j)*Ed0*(1-
alpha*X2_eq(2,1,j))/R/X2_eq(1,1,j)^2;
    J33(j)=Ag*u_in_eq/ttt;

    t5=Ag*u_in_eq+s*Dx*p_r*exp(-Er/R/X2_eq(1,1,j))*X2_eq(2,1,j);
    J41(j)=-Ag*u_in_eq*s*Dx*p_r*exp(-Er/R/X2_eq(1,1,j))*X1_eq(3,1,j)/t5^2;
    J42(j)=-Ag*u_in_eq*s*Dx*p_r*exp(-
Er/R/X2_eq(1,1,j))*Er/R/X2_eq(1,1,j)^2*X1_eq(3,1,j)*X2_eq(2,1,j)/t5^2;
    J44(j)=Ag*u_in_eq/t5;

    J52(j)=h*P*Dx/(rho_g*Ag*Cp_g*u_in_eq+h*P*Dx);
    J55(j)=rho_g*Ag*Cp_g*u_in_eq/(rho_g*Ag*Cp_g*u_in_eq+h*P*Dx);

    if (j==1)
        J3111=J311;
        J3122=J312;
        J3133=J313;
        J3144=J314;
    end

    %J21(j)=
     end;

X1_in_eq = X1_eq;

X2=X2_eq;

dtheta=zeros(N,1);
dtheta_new=zeros(N,1);
dTw=zeros(N,1);

As=zeros(2,2,N);
Bs=zeros(2,3,N);
Cs=zeros(3,2,N);
Ds=zeros(3,3,N);
```

```
% subroutine to place state space equations for each segment
for j=1:N

As1=J11t(j);
As2=J12t(j);
%As3=J21t(j);
As3=0;
As4=J22t(j);



% As(j)=[J11(j)-1.0 J12(j)
% J21(j) J22(j)-1.0];
As(:,:,j)=[As1 As2
    As3  As4];


Bs1=J13t(j);
Bs2=J14t(j);
Bs6=J25t(j);


%
% Bs(j)=[J13(j) J14(j) 0
% 0 0 J25(j)];

Bs(:,:,j)=[Bs1 Bs2 0
    0 0 Bs6];

Cs1=J31(j);
Cs2=J32(j);
Cs3=J41(j);
Cs4=J42(j);
Cs6=J52(j);

%
% Cs(j) = [J31(j) J32(j)
% J41(j) J42(j)
% 0 J52(j)];

Cs(:,:,j) = [Cs1 Cs2
    Cs3 Cs4
    0   Cs6];

Ds1=J33(j);
Ds5=J44(j);
Ds9=J55(j);
%
% Ds(j)=[J33(j) 0 0
% 0 J44(j) 0
% 0 0 J55(j)];

Ds(:,:,j)=[Ds1 0 0
    0 Ds5 0
    0 0 Ds9];


end



A=zeros(2*N,2*N);
```

```
B=zeros(2*N,3);
C=zeros(3,2*N);
D=zeros(3,3);


% Subrotines to make one large A, B, C, D matrices
for m=1:1:N
    A(2*m-1:2*m,2*m-1:2*m)=As(:,:,m);
    %for k=m-1:
    if (m>1)
    A(2*m-1:2*m,2*(m-1)-1:2*(m-1))=Bs(:,:,m)*Cs(:,:,m-1);

    ddd=Ds(:,:,m-1);

    for (k=m-2:-1:1)

        A(2*m-1:2*m,2*k-1:2*k)=Bs(:,:,m)*ddd*Cs(:,:,k);

        ddd=ddd*Ds(:,:,k);
    end
    end
end;


% %
for m=1:1:N
    B(2*m-1:2*m,:)=Bs(:,:,m);
    if m>1
        for k=m:-1:2
           B(2*m-1:2*m,:) = B(2*m-1:2*m,:)*Ds(:,:,k-1);
        end
    end
end

%
for m=1:1:N-1
    tttt=Ds(:,:,N);
    for k=N-1:-1:m+1
        tttt=tttt*Ds(:,:,k);
    end
    C(:,2*m-1:2*m)=tttt*Cs(:,:,m);
end
     C(:,2*N-1:2*N)=Cs(:,:,N);

 D=eye(3);
for m=N:-1:1
    D=D*Ds(:,:,m);
end


SYS=ss(A,B,C,D);   % Linearized system 2*N order

TF=tf(SYS);

[K,K1]=size(A);


% to make a Linear system when Tw and SV are fixed

A1=size(K/2,K/2);
B1=size(K/2,2);
C1=size(2,K/2);
```

```
D1=size(2,2);


for i=1:K/2
    for j=1:K/2
        A1(i,j)=A(i*2-1,j*2-1);
    end;
    B1(i,1)=B(i*2-1,1);
    B1(i,2)=B(i*2-1,2);
    C1(1,i)=C(1,i*2-1);
    C1(2,i)=C(2,i*2-1);
end;
D1=D(1:2,1:2);


SYS2=ss(A1,B1,C1,D1);      % Linear system if Tw and SV are fixed


% Reduction of order: Hankel norm minimization
[sys1,info1]=hankelmr(SYS2,1);
[sys2,info2]=hankelmr(SYS2,2);

% Reduction of order: Hankel norm minimization
[ssys1,info11]=balancmr(SYS2,1);
[ssys2,info22]=balancmr(SYS2,2);

% Transfer functions (1st and 2nd)
tf1=tf(ssys1);
tf2=tf(ssys2);

% Transfer functions (1st and 2nd)
tf1=zpk(tf1);
tf2=zpk(tf2);
```